ASPECTS OF 5G SYSTEM TECHNOLOGIES

by

Saad Mahboob

B.Sc., COMSATS Institute of Information Technology, Islamabad, 2005

M.Sc., Simon Fraser University, Burnaby, 2010

A research proposal presented to Simon Fraser University in partial fulfillment of

the requirement for the degree of doctor of philosophy

In the school of engineering science

Senior Supervisor:

Professor. Dr. Rodney Vaughan

Supervisors:

Dr. Lesley Shannon
Dr. Ash M. Parameswaran
Dr. Marek Syrzycki

Approval

Name:	**Saad Mahboob**
Degree:	**Doctor of Philosophy (ENSC)**
Title:	***Aspects of 5G System Technologies***

Examining Committee: **Chair:** Firstname Surname
Position

Rodney G. Vaughan
Senior Supervisor
Professor

Lesley Shannon
Supervisor
Associate Professor

Ash M. Parameswaran
Supervisor
Professor

Marek Syrzycki
Internal Examiner
Professor
Department of Mechatronic

Thomas Johnson
External Examiner
Associate Professor
School of Engineering, UBC

Date Defended/Approved: Month ##, ####

Ethics Statement

https://canvas.sfu.ca/courses/34125/users

The author, whose name appears on the title page of this work, has obtained, for the research described in this work, either:

a. human research ethics approval from the Simon Fraser University Office of Research Ethics

or

b. advance approval of the animal care protocol from the University Animal Care Committee of Simon Fraser University

or has conducted the research

c. as a co-investigator, collaborator, or research assistant in a research project approved in advance.

A copy of the approval letter has been filed with the Theses Office of the University Library at the time of submission of this thesis or project.

The original application for approval and letter of approval are filed with the relevant offices. Inquiries may be directed to those authorities.

Simon Fraser University Library
Burnaby, British Columbia, Canada

Update Spring 2016

ABSTRACT

The fifth generation (5G) of wireless connectivity is a global research effort for providing a significant jump in communications capacity. This will improve existing services for personal and business, navigation, and provide ultra-high-speed media distribution, etc. New applications will include wearable terminals, smarter homes, better vehicular safety and other critical infrastructure, and products that are currently unimagined. The 5G capabilities include higher reliability and data rates with lower latency, realized through new technologies such as (i) massive MIMO (multiple input, multiple output) - meaning the use of a large or massively large number of antennas, and (ii) higher carrier frequencies – meaning tens to hundreds of GHz - in order to have physically smaller antennas.

The massive MIMO is the most visible and compelling technology for 5G. The idea is to use massive arrays of elements in antennas for serving very large numbers of mobile terminals simultaneously. With 5G a cornerstone goal of current research in communications theory, radio-wave propagation, antennas, and electronics, new paradigms are being sought in many aspects of communications design and implementation. This particularly motivates a study of massive MIMO, with the aim of understanding and contributing to the knowledge pool for the communications performance expected from 5G. The breadth of technologies is too overwhelming to address within a single cover and so the following projects were selected are are presented in this thesis as contributions to 5G:

(i) an FPGA-based MIMO test-bed for experiments and proof-of-concept demonstrations of MIMO signal processing algorithms;

(ii) an advanced signal processing algorithm for massive MIMO antennas selection combining evaluated in a realistic propagation environment;

(iii) a design concept for a scalable distributed channel sounder, tested for indoor channel sounding.

Keywords: Massive MIMO, Software defined radio, FPGA, Convex optimization, Channel sounding, Optic fibre.

DEDICATION

This thesis is dedicated to my parents and late grandmother.

ACKNOWLEDGMENT

I owe a debt of gratitude to my supervisor, Dr. Rodney Vaughan, for his support and mentoring throughout my research work. I thank him, for his generosity for accepting me, at the hardest moment of my life (in words it is hard to describe). I am grateful to SFU to give me the opportunity of having worked with him. I acknowledge for the use of their facilities at the University of British Columbia.

I like to thank my external examiner Dr. Thomas Johnson for becoming part of my thesis committee. I also like to thank Dr. Ash M. Parameswaran, Dr. Marek Syrzycki and Dr. Lesley Shannon, for their valuable comments and the time they spent reading my thesis.

I thank the engineering science office staff for being so friendly and helpful. I thank my friends for the wonderful times I have spent with them. You have always made my days warmer and brighter.

Words are inadequate for me to express my gratitude to my family, especially to my mother. They have always cheered me on and always been there when I needed them. Thank you all.

TABLE OF CONTENTS

LIST OF FIGS

LIST OF TABLES

LIST OF ABBREVIATIONS

5G	Fifth Generation
ADC	Analog to digital converter
CBM	Correlation-based method
CFO	Carrier frequency offset
CLB	Configurable logic block
C-MIMO	Collocated multiple-input multiple-output
CSI	Channel state information
DAC	Digital to Analog converter
DCM	Distributed channel measurement
DCS	Distributed channel sounder
FPGA	Field programmable gate array
FUTON	Fiber optic networks for distributed extendible heterogeneous radio architectures and service provisioning
GEDOMIS	GEneric hardware DemOnstrator for MIMO Systems
HIL	Hardware in Loop
i.i.d	Independent and identically distributed
JTAG	Joint Test Action Group
LOS	Line of sight
LSF	Large scale fading
MEA	Multiple element antenna
MIMO	Multiple-input multiple-output
NBM	Norm-based method
OFDM	Orthogonal frequency division multiplexing
P2MP	Point to multiple points
PDP	Power delay profile
PN	Pseudorandom noise
RAU	Remote antenna unit
RF	Radio frequency
RoF	Radio-over-fiber
Rx	Receiver
SDR	Software-defined radio
SINR	Signal to interference and noise ratio
STBC	Space-time block codes
Tx	Transmitter
USRP	Universal software radio peripheral
VHDL	Verilog hardware descriptive language
VSA	Vector signal analyser

CHAPTER 1: INTRODUCTION

1.1 Motivation

Mobile communications, developed over the last century, has been a triumph of electrical engineering. Currently we are enjoying and marvelling at what is widely referred to as the fourth generation (4G) of cellular systems. The next generation of wireless communication will support another major growth cycle for mobile users and the data sizes and rates associated with their demand. Two 5G technologies that are under the spotlight are *massive MIMO* and *millimetre wave communication.* The mmwave frequencies allow the sizes of antennas, and in particular massive numbers of them in arrays which can be physically smaller than using currently deployed frequencies. Antennas, *per se,* are not investigated here - the 5G focus of this thesis is on aspects of massive MIMO communication systems which operate on current frequencies below 6GHz. This allows physical measurements for a reasonable cost, and comparisons with existing technologies. Massive MIMO is a key technology that will enable 5G to significantly increase network capacity and spectral efficiency, improving the end-user experience [1]. Some of the characteristics of massive MIMO include all-digital signal processing and channel hardening. However, the use of analogue processing at the radio frequencies will survive in some form because much of that processing is inherently analogue. An example is the switches used for preselection of antennas in massive MIMO, addressed in Chapter 2. The baseband processing, including much of the simultaneous combining of antenna signals that follows preselection, will be purely digital. *Channel hardening* is a recent term for the traditional diversity action available from using multiple antennas: the combined signal has a lower variance, which approaches zero as the number of antennas approaches infinity. Over the last the couple of years, massive MIMO has gone from being a theoretical concept for channel hardening to becoming a promising key ingredient for 5G. This

breath-taking pace of technology development is motivated by the fact that it provides a way to increase the capacity and capacity efficiency by “simply” upgrading existing base stations. In short, massive MIMO is rapidly approaching technical, and even commercial, feasibility. The goal in round numbers is as follows: to provide a hundred times higher capacity efficiency without installing a hundred more base stations [1].

The objective of this thesis has been to seek an understanding of some key aspects of massive MIMO technology. (To address all aspects of 5G does not seem feasible under a single cover.) To do so, three projects have been undertaken:

(i) developing an antenna selection algorithm for massively MIMO antennas system,

(ii) designing and demonstrating a scalable distributed channel sounder, and

(iii) implementing a MIMO signal processing algorithm on a Software Defined Radio (SDR) digital signal processing platform.

These projects are described in subsequent chapters, following this introduction.

1.2 Background

Massive MIMO is essentially a scaled-up version of conventional MIMO. This scale-up is about an order magnitude compared to current state-of-the-art, in terms of capacity, and number of antennas, etc. This in turn follows the *scale-up basis of 5G*, which is often mentioned in the literature to be a factor of a thousand, relative to 4G. Massive MIMO indicates the use of antenna arrays with a few hundred antennas, simultaneously serving many tens of terminals in the same time-frequency resource. The basic premise behind massive MIMO is to reap all the benefits of conventional MIMO, but on a much greater scale [1].

The question arises as to what is “conventional MIMO”?. The term MIMO is used for any system that uses multiple antennas at either one end or at both ends of a link, so this includes traditional antenna diversity, and in fact MIMO and antenna diversity can be used interchangeably. For this thesis, the conventional MIMO is

taken to be 2-by-2 antennas (two antennas at each end of the link), using Alamouti 2-by-2 space-time coding. So this is not “full MIMO”, in the sense of an orthogonalization of the channels into eigen-channels, which, once the eigen-channels are established, gives the greatest capacity available in a mathematical sense. Deploying eigen-MIMO requires channel knowledge at the transmitter, which in turn means that the channel resource, i.e., the very metric being maximized, must be consumed in order to sound the channel and then interchange the information to the transmitters. For fast-changing channels, the act of getting the channel knowledge (or channel state information - CSI) to the transmitters can dominate the channel usage and compromises the useful capacity for a practical situation. For slow-fading channels, the sounding requirements are also slow, and require less capacity resource. Consequently, channel sounding ideas suitable for MIMO systems are required. In a communications link the channel sounding can buried in the signal processing in the form of pilot symbols, and then a protocol for interchanging the CSI if that is required at the transmitter, as in the case of eigen-MIMO. The CSI is not required in space-time coding. There are several space-time codes available, ranging from 2-by-1 to 8-by-8, and these codes are mostly hand-crafted, although super-computer searches continue to seek new ones. The question remains as to how to estimate the channels in order to evaluate the operation of a proposed deployment (without actually undertaking the deployment of course), and one idea for solving this is investigated as part this thesis (Chapter 3).

Because massive MIMO is a scaled up version of conventional MIMO, its development heavily relies on established MIMO theory [1], [2]. The most significant MIMO achievements include the pioneering work, such as that presented in [3], where the available mathematical capacity was shown to linearly increase with the minimum number of the transmitting or receiving antennas, over Gaussian noise and Rayleigh fading links. (In fact this result was also shown by J.Winters in an earlier publication) This result, along with the invention of space-time coding, for example by Alamouti, have transformed the expected capacity performance of a link in less than a few of decades. The performance advantage

of MIMO is measured by metrics such as diversity gain [4], [5] and multiplexing gain [1] - [6], and of course various capacities (mathematical forms to practicable forms), are applicable to massive MIMO as well.

The following diagram (Figure 1) gives an indicative view of the deployment of massive MIMO for an outdoor situation. It depicts linear arrays, often comprising basic elements spaced by a small electrical distance (normally less than a wavelength) which can be mounted on the roof or wall of a building in order to illuminate an angular field-of-view of up to a hemisphere. Cylindrical arrays can be used for circular coverage. Finally, Figure 1 also depicts distributed antennas – where the elements (or subarrays) are spaced by a very large electrical distance - in the case of Figure 1, around a building roof.

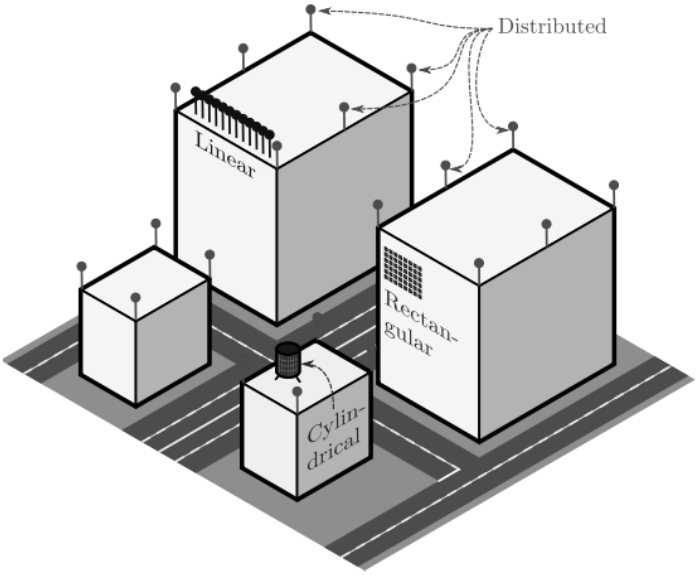

Fig. 1.1. Configurations of massive MIMO system. (Copied from [7]**)**

Other distributed antenna systems (DAS) have larger separations, compatible with traditional macro-diversity, where the antennas are spread out to be different base station sites that have independent lognormal, or shadow, fading, for any user in the coverage areas. The advantage of DAS is the larger (geographic) coverage compared to conventional arrays, and the disadvantage is the need for electrically long, low-loss, fast, radio-frequency coherent connections between the spaced

antennas. This is the same as the array feed problem (the feed system is typically a much higher cost and greater source of loss, than the set of antenna elements comprising the array antenna itself) but on an exaggerated spatial scale. Therefore, new ideas are required for this feed, and one such idea is developed and demonstrated in this thesis (Chapter 4).

1.3 Literature summary

This section gives a short overview of the literature pertinent to the three projects of massive MIMO. The following questions are addressed as three projects on massive MIMO in this thesis.

(1) How to select antennas in a massive MIMO communication system?

The first research problem focuses on developing an antenna selection algorithm for massive MIMO. It relates to the "feed problem" mentioned above – namely that the feed system is often the dominant cost in an array. In a massive array, the feed problem becomes massive. The antennas themselves are relatively inexpensive, so if we can reduce the feed costs by simultaneously using only some of the massive array, then there may be a hardware advantage. Therefore, a way forward is required for choosing those elements for simultaneous signal combination, a process that is referred to here as *preselection*. We present an antenna preselection scheme based on capacity maximization for downlink transmission. Considerable work has appeared in the literature regarding antenna selection algorithms for collocated MIMO. (Strictly speaking, *collocated* is an incorrect term in an antenna context, because the antennas are *closely spaced* in a conventional array, which is different to *collated antennas* which would also have collocated feeds - such as three orthogonal dipoles for three-branch polarization diversity). There is little work done on antenna selection in massive MIMO. Prior work on antenna selection has focused mostly on collocated MIMO (again using the term as used in the literature) [8], [9], [10], [11], [12], [13]. Antenna *selection* is a generalization of selection diversity, where a single antenna, or diversity branch, with the maximum instantaneous channel gain, or some other communications

quality metric, is used for the selection action. For preselection, we seek to select several of the elements of an array, which can then be used for non-selection signal combining. The optimum algorithm to select N of M antennas is exhaustively searching over all possible antenna combinations and selecting the one that yields maximum capacity. This method is not feasible, in the general case, due to the computational complexity. Various algorithms for conventional MIMO [8], [9], [10], [11], [12], [13] have been extended to massive MIMO systems, and some new analysis have been undertaken for massive MIMO antenna selection, eg., [13], [14], [15].

(2) How to implement an FPGA based radio-over-fibre (RoF) MIMO-OFDM communication system?

As wireless communication systems are increasingly using multiple antenna techniques, not only is the feed problem is coming more to the fore, but the signal processing requirements are also increasing. The idea is to use fibre optic connections for the feed between distributed antennas, and FPGA-based algorithms, and a demonstration is required to identify its utility.

Due to the wide variety of available MIMO algorithms for different types of MIMO systems, with their different complexities and numerical behaviour using fixed-point implementations, realizing algorithms – typically on FPGAs - is a challenging task. This project seeks to understand aspects of the practical signal processing engineering by developing a block-based (meaning blocks of multiple symbols) algorithmic description composed of coarse-grain (meaning symbol-rate processing) functions to found the design process. This project uses a modular implementation approach (meaning different FPGA IP-cores), which preserves the structure of the MIMO algorithm while maintaining a connection between the algorithm, the signal processing flow, and the physical architecture. The idea is to learn about bridging the gap between a theoretical-only understanding of MIMO algorithms and their practical implementation on FPGA-based software-defined radio (SDR) platforms. FPGAs allow higher processing power compared to other

platforms such as powerful commodity-type computers (laptops and PCs). Various authors have discussed the hardware implementation of MIMO, but most of the literature that focuses on FPGA implementations lack complete real-time setup. Nevertheless, there are some interesting publications on real-time implementation of various MIMO algorithms inside the FPGA for testbeds.

A summary of published testbeds is as follows. [16] describes the details of the "Vienna" MIMO test-bed. The signal processing algorithms are implemented in MATLAB (i.e., not in an FPGA). The transmission data is generated stored in PC and then transmitted using the RF module connected to the computer. The transmit and receive PCs are controlled using a LAN connection. This platform supports a 4x4 MIMO capability. [17] discusses a MIMO test-bed developed at the University of Duisburg-Essen, Germany. This test-bed uses the Sundance hardware [18] for baseband processing (such as coding/modulation schemes including OFDM and CDMA) with RF modules by Amtel Inc. [18]. The GEDOMIS (GEneric hardware DemOnstrator for MIMO Systems) in [19], [20], describes a complete real-time multi-antenna experimental 4x4 MIMO-OFDM transmission system operating in two ISM bands. The system enables evaluation of the physical layer baseband algorithms targeting the MIMO systems on the FPGA platform. The focus is on the impact of using increasing bandwidth, which scales the implementation complexity of the baseband signal processing algorithms. The system was successfully demonstrated under realistic channel conditions in static scenarios (non-mobile channels). In [21], a low bandwidth FPGA-based MIMO test-bed is used to carry out a channel measurement campaign to analyze its capacity, and evaluate experimentally a pilot-based channel estimation scheme on the FPGA. [22] presents a real-time FPGA prototype for a 4 by 1 MIMO-OFDM transceiver in a 20 MHz bandwidth. FPGA implementation and results are reported along with measurements that demonstrate the throughput of spatial multiplexing with four spatial streams.

(3) How to realize a channel sounder based upon a test-bed system that is suitable for Distributed Antenna Systems (DAS)?

Even though a remarkable amount of research in MIMO systems has been conducted over the past two decades, the full potential of MIMO systems is yet to be exploited in practical applications. One reason for this is a shortfall of understanding of the characteristics of radio channels. Therefore, the radio channel characteristics should be investigated more thoroughly, and in fact this is always a cornerstone step for configuring and designing a wireless system. Several challenges are associated with the development of a distributed channel sounder. The basic tool is the two-port Vector Network Analyzer (VNA), which can measure a basic channel (the scattering parameter S_{21} is related to the transfer function of a single channel.) The challenge is that a large number of channels need to be sounded simultaneously, and most VNAs are two-port only, although some 4-port versions are available (with 3-4 receivers for simultaneous measurement). However, the cost of a multiport test is formidable. The alternative is to make a multiplexer, which allows multiple channels to measured in sequence. But for changing channels, and a lot of them, the measurement does not supply appropriate information because of the non-simultaneous nature of the measurements. For example, the instantaneous correlation between different links has a significant impact on the performance of distributed MIMO systems. Although the calculation of this correlation is not addressed in this thesis (and is a relatively straightforward calculation once sounding data has been obtained), a new concept for how to simultaneously sound multiple channels is presented. The prior work on channel sounders appears limited to [23], [24], [25], [26], [27], [28], [29], [30], [31], [32] [33], [34]. None of these offer the elegance of the presented concept, which uses a “regular” two-port VNA plus a set of optical-fibre-based delays, to sound channels simultaneously. With more optical fibre delays, more channels be sampled. Our demonstration is limited to 3 channels. While the optical hardware can be expensive (tens of thousands of dollars), but this is small compared to using many-port VNA test sets. Optical systems are increasingly

being used with VNAs and radio frequency testing, so the optical component costs are plummeting.

1.4 Published and Submitted Contributions from this thesis

The published contributions of this work are as follows.

1. S. Mahboob, R. Ruby, and Victor C.M. Leung., “Transmit antenna selection for downlink transmission in a massively distributed antennas system using convex optimization”, in *Proc. IEEE International Conference on Broadband And Wireless Computing, Communication and Applications*, pp. 228-233, 2012.
2. S. Mahboob, and R.G. Vaughan, “Fiber-Fed distributed antenna system in an FPGA software defined radio for 5G demonstration,” *IEEE Transactions on Circuits and Systems,* pp. 1-5, publication date April, 2019.
3. S. Mahboob, and R.G. Vaughan, “Antenna selection in a massive MIMO,” *IEEE Transactions on Circuits and Systems--II*, (Submitted, September 2019).
5. S. Mahboob, S.B. Ram, R.G. Vaughan, “Vector channel sounder using fiber delay lines to separate the channels”, *Proc. IEEE International Symposium on Antennas and Propagation and USNC-URSI National Radio Science Meeting*, pp. 1113- 1114, 2017.
6. R. Ruby, S. Mahboob, and D.G. Michelson, “Optimal configuration of distributed MIMO antennas in underground tunnels”, *IEEE International Symposium on Antennas and Propagation and USNC-URSI National Radio Science Meeting*, pp. 65-66, 2014.
7. S. Mahboob, Rukhsana Ruby, David G. Michelson and Victor C.M. Leung., “Antenna Selection in Massively Distributed Antenna Systems for Short Range Vehicular Networking Infrastructure”, (Poster) *Presented at 4th Annual Workshop on Developing Next Generation Intelligent Vehicular Networks and Applications* (DIVA), 2014-Ottawa Canada.

8. S. Mahboob, Roberto Rosales, David G. Michelson and Victor C.M. Leung, “A Distributed Channel Sounder for Short Range Vehicular Networks in Urban Microcells”, (Poster) DIVA, 2014- Ottawa Canada.

1.5 Organization of Thesis

The thesis is organized as follows. In Chapter 2, we discuss the antenna preselection in a massive MIMO downlink environment. This includes an interior-point algorithm from convex optimization theory. In Chapter 3, we present a vector signal analyzer (VSA) based distributed channel sounder (DCS), with radio over fibre (RoF) connected to remote antenna units (RAUs), also demonstrating measurements for (indoor) distributed channel sounding. This measurement approach has the potential for massive MIMO channel measurements, and this is a unique feature – there is no other technology approach that can undertake this measurement (viz., a simultaneous measurement) that is feasibly priced. The proposed channel sounder technique was developed and an experiment undertaken to prove the concept. In Chapter 4, a radio-over-fibre system is developed for a 2 by 2 Alamouti space-time coded MIMO-OFDM system, implemented in an FPGA. The motivation is recalled as striving to understand the hardware level architecture and engineering. Also in mind here was the need for scalable system. (Meaning that these 2 by 2 modules could be concatenated into a massive MIMO system.) The complete transmit and receiver is developed in the FPGA fabric using Verilog, Xilinx System Generator and C programming. Chapter 5 concludes the thesis, with some future directions for research in massive MIMO.

CHAPTER 2: ANTENNA SELECTION IN A MASSIVE MIMO USING CONVEX OPTIMIZATION

2.1 Overview

In recent years, due to the increasing demand of the data transmission rate, a lot of research based on Multiple-Input Multiple-Output (MIMO) system has been produced. MIMO systems can increase the system capacity and improve transmission reliability, etc., however, the multiple RF chains associated with multiple antennas are costly in terms of size, power and hardware. Antenna preselection (also referred to hereon simply as selection)is a signal processing technique that helps to reduce the system complexity and cost of the RF front-ends. This chapter describes the concept of antenna preselection in a single-user massive-MIMO system. In this work, convex optimization is used to select the optimal number of antennas, to achieve the best compromise between the achievable capacity and system complexity. Specifically, the interior-point algorithm from optimization theory is utilized.

MIMO requires a multi antenna setup at the base-station [7]. For example, the LTE standard allows only up to 8 antennas at the base-station. It is documented in [35] [36] that massive-MIMO can reduce the inter-cell interference between users, using the same frequency resource. This happens since as the number of base-station antennas grow, the channel vectors between the users and the base-stations become very long random vectors [2], [37], [1] and under **"**favourable propagation conditions" (a misleading description of the situation, but widely used in the MIMO signal processing literature) , these channel vectors become pairwise orthogonal [3]. As reported in [38], [39], under the favourable propagation conditions, even a simple linear precoding/detection scheme e.g. zero-forcing and matched filtering, becomes nearly optimal. Other attractive features of massive-MIMO are simple hardware, making it possible to deploy a large number of antennas. So far, investigations are based on the theoretical independent and identically distributed (i.i.d.) complex Gaussian, i.e. Rayleigh fading channels. With a very large antenna array, things that were random before starting to look

deterministic [40]. Therefore, the effect of small-scale fading is averaged out. Furthermore, when the number of BS antennas grows large, the random channel vectors between tfhe users and the BS become pair-wise orthogonal [1]. In the limit of an infinite number of antennas, with simply matched filter processing at the BS, uncorrelated noise and intra-cell interference disappear completely [41]. Massive-MIMO has other advantages as well, e.g., eliminating the effect of uncorrelated noise and fast fading. For a massive MIMO, the real expense comes from the RF-chain associated with each antenna. The RF-chain comprises of LNA, mixer and an analog-to-digital (ADC) and digital-to-analog (DAC) convertors. One solution, to reduce the cost is antenna selection, that can reduce the cost of RF chains, yet preserves diversity and multiplexing gains obtained from the actual system. With a limited number of RF chains and more antennas, antenna selection improves the system performance by exploiting the spatial selectivity, as the subset of antennas with the best channel conditions is selected and switched to RF chains [42] [43].

2.2 Background

Prior work on antenna selection is focused mostly on conventional MIMO (with small number of antennas e.g. 2, 4, 8). Antenna selection in MIMO can be considered as a generalization of selection diversity [44], where a set of antennas with maximum instantaneous channel gains is selected. Antenna selection algorithms are categorized based on the selection criteria. Commonly used criteria are either maximization of channel capacity or maximization of signal-to-interference-plus-noise ratio (SINR) at the receiver [45]. In conventional MIMO systems, the optimum algorithm to select antennas is exhaustively searching over all possible antenna combinations, i.e., calculating determinants for each channel instance, and selecting the one that yields maximum capacity. This method is not feasible due to computational complexity. The norm-based method (NBM) [46] is a suboptimal antenna selection approach that selects the transmit antennas corresponding to the columns of channel gain matrix with the largest Euclidean norm. Although simple and computationally efficient, NBM incurs capacity-loss as

it is sub-optimal. The correlation-based method (CBM) [47] searches columns in the channel matrix with the largest correlation and deletes ones with the lowest power. A near-optimal antenna selection algorithm based on capacity maximization is presented by Gorokhov [48]. It uses matrix inversion as a recursion for capacity computation, which increases its complexity. Decremental antenna selection approaches are presented in [48] and [10], which begin with a complete set of antennas and remove one antenna per iteration. In each step, the antenna with the lowest contribution to the capacity is removed. This process is repeated till columns are eliminated. The algorithm proposed by Alkhansari [49] gives a near optimal antenna selection at reduced complexity. The algorithm starts with an empty set and adds antennas iteratively based on its capacity contribution. Algorithms [8] and [49] are categorized as incremental antenna selection approaches. [50] and [51] present the antenna selection approaches in multiuser scenarios, using the block-diagonalization and dirty-paper coding. Researchers have addressed the topic of antenna selection in the massive-MIMO system, e.g. [14] [52] [53] [54] [55] [56] [57] [58] [59] have described various antenna selection algorithms in massive-MIMO systems. When the circuit power is considered, the question of how to perform antenna selection to improve energy efficiency is investigated in [60] and [61]. In [60], the RF chain selection for configurations both with and without CSI is studied to maximize spectral efficiency for a given total power consumption constraint. It is shown that for MISO without CSI, the optimal number of RF chains is about half the maximum number of RF chains that can be supported by the power budget. In [55], channel capacity based on antenna selection is derived, and the variance of the mutual information is found to decrease as the number of antennas increases. This work also shows that to maximize the energy efficiency, all antennas should be used if the circuit power can be ignored compared to the transmit power while only a subset of the antennas should be chosen if the circuit power is comparable to the transmit power.

2.3 System Model

Consider the downlink of a massive MIMO system shown in Fig. 2.1. The system includes one BS equipped with an array of M antennas that receive data from K single antenna users. The users receive their data in the same time-frequency resource. The downlink propagation channel is,

$$G = HD^{1/2} \tag{1}$$

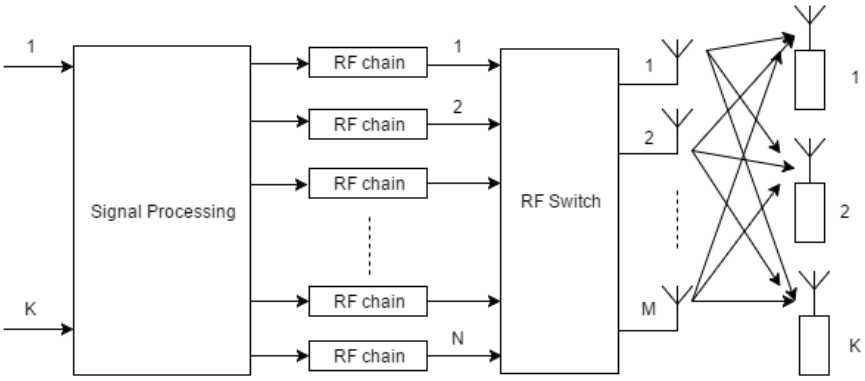

Fig. 2.1. System model of Massive MIMO system.

where D is the large-scale fading (LSF) matrix and H accounts for the small-scale fast fading usually modelled by Rayleigh distribution. The LSF matrix is diagonal, with elements account for the effects of propagation-loss and lognormal shadowing. The lognormal shadowing is assumed independent at each antenna and varies slowly with time. The fast fading coefficients, i.e., elements of H are assumed independent and identically distributed random variables with a zero mean and unit variance. The dimensions of H and D are $K \times M$ and $M \times M$, respectively. The channel matrix G models independent fast fading, geometric attenuation, and log-normal shadow fading. The channel g_{km} is,

$$g_{km} = h_{km}\sqrt{\beta_k} \qquad m = 1, 2, \ldots, M \tag{2}$$

where h_{km} is the fast-fading coefficient from the m^{th} antenna of the BS to the k^{th} user. $\sqrt{\beta_k}$ models the geometric attenuation and shadow fading which is constant

over many coherence time intervals. This assumption is reasonable since the distances between the user and the BS is much larger than the distance between the antennas, and the value of β_k changes very slowly over time. H is the $K \times M$ matrix of fast-fading coefficients between the K users and the BS, i.e. $[H]_{km} = h_{km}$ and D is a $K \times K$ diagonal matrix, where $[D]_{kk} = \beta_k$. We assume that the BS has perfect CSI. For simplicity, we assume equal power allocation among the users i.e. $P = \frac{1}{K}$ and select the M antennas that maximize the channel capacity.

2.4 Favourable Propagation in a Massive MIMO

We assume that the fast fading coefficients i.e. the elements of H are i.i.d RVs with a zero mean and unit variance. Then applying the above two conditions on any two columns p and q inside the matrix G. In this case, we have

$$\left(\frac{G^H G}{M}\right)_{M \gg K} = D^{1/2} \left(\frac{H^H H}{M}\right)_{M \gg K} D^{1/2} \approx D \quad \textbf{(3)}$$

Clearly, if all the fading coefficients are i.i.d. and zero mean, we have approximately favorable propagation. Recent channel measurements campaigns have shown that massive MIMO systems have characteristics that approximate the favorable propagation assumption fairly well [4], and therefore provide experimental justification for this assumption. For each use of the channel, the massive MIMO transmits a $M \times 1$ vector s_f, and the users receive a vector signal x_f. The received signal is represented as,

$$x_f = \sqrt{\rho_f} G s_f + w_f \quad \textbf{(4)}$$

The term w_f is a $K \times 1$ noise vector at the receiver, whose components are independent and identically distributed zero-mean circularly symmetric complex Gaussian with unit variance. ρ_f in (4) denotes the signal-to-noise ratio (SNR). The

capacity of massive MIMO is represented as [2],

$$C_{M\gg K}(G) = \log_2 \det\left(I_M + \rho_f G^H G\right) \approx \log_2 \det\left(I_M + \rho_f M\, D\right) \quad \textbf{(5)}$$

In this expression, we assume that the massive-MIMO allocates equal power to all the terminals. If the BS assigns different powers to various antennas, the expression becomes,

$$C_{M\gg K}(G) = \log_2 \det\left(I_M + \rho_f M\, PD\right)$$

where P is a diagonal matrix with power allocation $(p_1, p_2, \ldots, p_k)$ as its diagonal elements. Here, we assume it as an identity matrix for simplicity.

2.5 Antenna Selection as a Convex Problem

If we are to select N optimal antennas from the M available ones, the massive MIMO capacity in (5) no longer remains a function of G but instead becomes a function of the antennas chosen. We formulate the transmit antenna selection problem in massive-MIMO as a linear programming problem, and solve it using the interior-point algorithm. Linear programming is a mathematical optimization technique to solve a linear objective function, subjected to linear equality and linear inequality constraints. Its feasible region is a convex polyhedron. A linear programming problem is convex in nature, so any local optimum is the global optimum [62].

It is well known that for any linear objective function, the optimum only occurs at one of the corners (vertices) of the feasible polygon region [63] [62]. Define $\Delta_i \ (i=1,\ldots,M)$ as antenna selection variable such that,

$$\Delta_i = \begin{cases} 1 & i^{th}\ antenna\ selected, \\ 0 & otherwise \end{cases} \quad \textbf{(6)}$$

Now consider a $M \times M$ diagonal matrix Δ used for antenna selection at the CU, which has Δ_i as its diagonal entries. The diagonal matrix Δ is represented as,

$$\mathbf{\Delta} = \begin{bmatrix} \Delta_1 & & & \\ & \Delta_2 & & \\ & & \ddots & \\ & & & \Delta_{M\times M} \end{bmatrix}_{M\times M} \quad \textbf{(7)}$$

where Δ_i is defined as in (6). Denote $F = G\Delta$ as the $K \times M$ modified channel-gain matrix [63]. Using (5), the modified capacity equation for the massive MIMO can be rewritten as,

$$\begin{aligned} C_{M \gg K}(G) &= \log_2 \det\left(I_M + \rho_f F^H F\right) \\ &= \log_2 \det\left(I_M + \rho_f M \Delta P D\right) \end{aligned} \quad \textbf{(8)}$$

Eqn. (8) follows from the fact that $\Delta^{\mathrm{H}}\Delta = \Delta$. The capacity equation in (8) is concave in Δ_i, where $i = 1, \ldots, M$ [63]. A function $f(\mathrm{X}) = \log_2 \det(\mathrm{X})$ is concave in the entries of X if X is a positive definite matrix. The concavity of the function f is preserved under the affine transformation. The optimization problem for antenna selection is,

$$\begin{aligned} \underset{\{\Delta\}}{\text{maximize}} \quad & C(\mathbf{\Delta}) = \log_2 \det\left(I_M + \rho_f M \Delta P D\right) \\ \text{subject to} \quad & \Delta_i \in \{0,1\} \\ & trace(\Delta) = \sum_{i=1}^{M} \Delta_i = N \end{aligned} \quad \textbf{(9)}$$

Since the variables Δ_i are integer variables, this makes the antennas selection in massive MIMO an integer programming problem. We use the concept of linear programming relaxation to solve (9) [62]. Linear programming relaxation of the 0/1 integer program arises by replacing the constraint that each variable must be 0 or

1, by a weaker constraint such that each variable is a real number within the interval [0, 1], i.e., for each constraint of the form, $\Delta_i \in \{0, 1\}$ of original integer program, one instead uses a pair of linear constraints $0 \le \Delta_i \le 1$. The relaxation technique transforms the integer programming problem into a linear program that is solvable in polynomial time [62]. Applying this technique, the antenna selection problem in the massive MIMO can be expressed as,

$$\begin{aligned} &\underset{\{\Delta\}}{\text{maximize}} \quad C(\boldsymbol{\Delta}) = \log_2 \det\left(I_M + \rho_f M \Delta P D\right) \\ &\text{subject to} \quad 0 \le \Delta_i \le 1 \\ &\qquad\qquad trace(\Delta) = \sum_{i=1}^{M} \Delta_i = N \end{aligned} \qquad \textbf{(10)}$$

This optimization problem yields a fractional solution, from which the N largest Δ_is are selected and their indices represent the optimal transmit antennas. Since $\log(\cdot)$ is an increasing function, for ease of analysis, we remove the logarithm in front of the objective function in (10). In addition, by inserting a negative sign on the objective function, we have turned our optimization problem into an equivalent minimization of the objective function. We have two constraints and therefore introduce the Lagrange multiplier λ in the objective function to make it unconstrained minimization problem. The unconstrained objective function is denoted

$$F = -\det\left(I_M + \rho_f M \Delta P D\right) + \lambda \left(\sum_{i=1}^{M} \Delta_i - N\right) \qquad \textbf{(11)}$$

$$\begin{aligned} &F = -\left(1 + d_1\Delta_1\right)\left(1 + d_2\Delta_2\right)\ldots\left(1 + d_M\Delta_M\right) + \\ &\lambda \left(\sum_{k=1}^{M} \Delta_i - N\right) \end{aligned} \qquad \textbf{(12)}$$

where d_i is the product of ρ_f , M and the i^{th} element of the channel gain matrix D. The gradient of the objective function is a vector of dimension M. The i^{th} element of this vector is,

$$\frac{dF}{d\Delta_i} = -d_i\left(1+d_1\Delta_1\right)\left(1+d_2\Delta_2\right)\ldots\left(1+d_{i-1}\Delta_{i-1}\right)+ \left(1+d_{i+1}\Delta_{i+1}\right)\ldots+\lambda \quad \textbf{(13)}$$

The Hessian of the objective function F is a $M\times M$ matrix Ω with all diagonal elements zero, given by

$$\Omega = \begin{pmatrix} 0 & \Omega_{1,2} & \ldots & \Omega_{1,M} \\ \Omega_{2,1} & 0 & \ldots & \Omega_{2,M} \\ \vdots & \vdots & \ddots & \vdots \\ \Omega_{M,1} & \Omega_{M,2} & \ldots & 0 \end{pmatrix} \quad \textbf{(14)}$$

$$\Omega_{1,2} = -d_1 d_2\left(1+\Delta_3 d_3\right)\ldots\left(1+\Delta_M d_M\right)$$

$$\Omega_{1,M} = -d_1 d_M\left(1+\Delta_3 d_3\right)\ldots\left(1+\Delta_{M-1} d_{M-1}\right)$$

etc. This matrix is a positive semi-definite under the constraint $0\le\Delta_i\le 1$, and thus the problem is convex and there exists a global optimal for this problem. We can use MATLAB to find the optimal solution to this problem.

2.6 Complexity Analysis

The average complexity measured in terms of an average number of floating-point operations (flops) is used. Simulations were performed in MATLAB, in which the number of flops equals 2 for complex addition and 6 for multiplication. For real numbers, both addition and multiplication require 1 flop. We have compared the computational complexity of various algorithms. In exhaustive searching (ESA), the computational complexity of determinant is $1/3\times n^3$ (complex multiplications

and additions) for $n \times n$ matrix. There are $\binom{M_T}{N_T} \times \binom{M_R}{N_R}$ determinants. The total number of complex multiplications and additions required will be $\binom{M_T}{N_T} \times \binom{M_R}{N_R} \times 1/3 \times n^3$ where $n = \min\{N_T, N_R\}$. This exhaustive search grows exponentially with the number of antennas in a massive-MIMO system. This is evident from Stirling's approximation of factorial [63],

$$M! = M^M e^{-M} \sqrt{2\pi M} \quad \textbf{(15)}$$

In the technique described in [12], the upper bound of receive antenna selection is $O\left(M_R^{N_R}\right)$ and for transmit antenna selection $O\left(M_T^{N_T}\right)$. The upper bound for joint transmit and receive antenna selection is $O\left(M_R^{N_R} M_T^{N_T}\right)$. Similarly, antenna selection algorithm [10] will require $\binom{M_T}{N_T} + \binom{M_R}{N_R}$ determinants and $\binom{M_T}{N_T} + \binom{M_R}{N_R} \times 1/3 \times n^3$ complex additions and multiplications, where $n = \min\{N_T, N_R\}$. Similarly, fast antenna selection from [44] is bounded by $O\left(N_T M_T^2\right)$ for the transmit antenna selection. If we use the Karmakar's Interior Point Method (Barrier Method) to solve (10), the number of Newton steps is upper bounded by $\sqrt{M}$ [63]. The total complexity is $O\left(M^{3.5}\right)$. The number of Newton steps does not increase with increasing M [62]. This complexity is comparable to

the $O\left(M^3\right)$ complexity of [15]. The pseudo-codes of Barrier method is listed in Table 2.1.

TABLE 2.1

The barrier method [26] – $O\left(M^{3.5}\right)$

Given strictly feasible $\Delta_i\ (i=1,\ldots,M)$, $t=t^{(0)}\succ 0$, $\mu>1$ (update parameter), $\in>0$ (tolerance), **repeat** the following steps:

1. Compute $\Delta_i^*(t)$ by minimizing $t\, f_o(\mathbf{\Delta})+\phi(\mathbf{\Delta})$ subject to $\sum_{i=1}^{M}\Delta_i=N$, starting at Δ_i using the Newton method
2. Update $\Delta_i:=\Delta_i^*(t)$ $(i=1,\ldots,M)$
3. If $M/t\prec\in$, **stop** else update $t:=\mu t$

Here,

$$f_o(\mathbf{\Delta})=-C_r(\mathbf{\Delta})$$

$$\phi(\mathbf{\Delta})=-\sum_{i=1}^{M}\log\left(\Delta_i(1-\Delta_i)\right)$$

2.7 Simulation Results

In this section, the above preselection algorithm (with the interior point method) is evaluated firstly for a small number of antennas (M=16, N=4, K=1) to allow comparison with existing techniques. The ergodic asymptotic capacity is the performance metric, estimated by averaging over 10,000 independent realizations of the Rayleigh channel gain (there is no lognormal shadow component, again to allow comparison with existing results). The results are in Fig.2: the optimal result from exhaustive search; the results calculated from the norm-based selection (NBS) method; from the fast algorithm of [8]; and from a "random preselection".

The random preselection is the same as combining M=4 antennas with no preselection, and serves as a check, since results are known for purely Rayleigh channels. Fig.2.2 shows that the capacity from our method is very close to that of the optimal selection. The NBS method, while having a particularly low complexity, performs only marginally better than for the case of no selection. The reason is that it tends to select the antennas that have the same fading coefficients during different iterations (so it is better suited to slower fading) [9]. The exhaustive search requires multiplications and is only feasible here because of the small number of antennas (takes about 15 minutes on a current PC per iteration, and only 100 results were used for the averaging). The "optimal selected" results agrees with that presented in [49], which serves as another check.

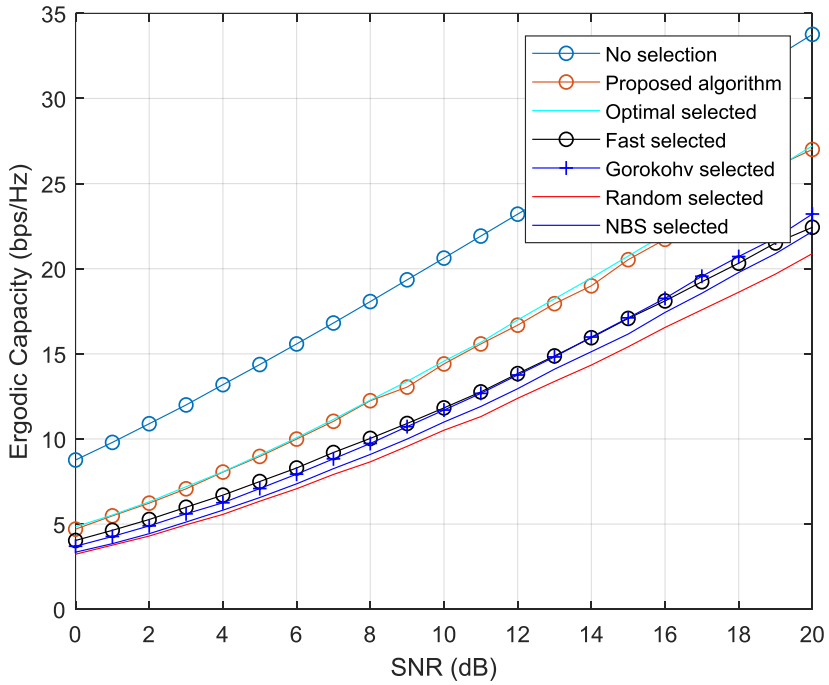

Fig. 2.2. Comparison of proposed antenna selection to conventional techniques.

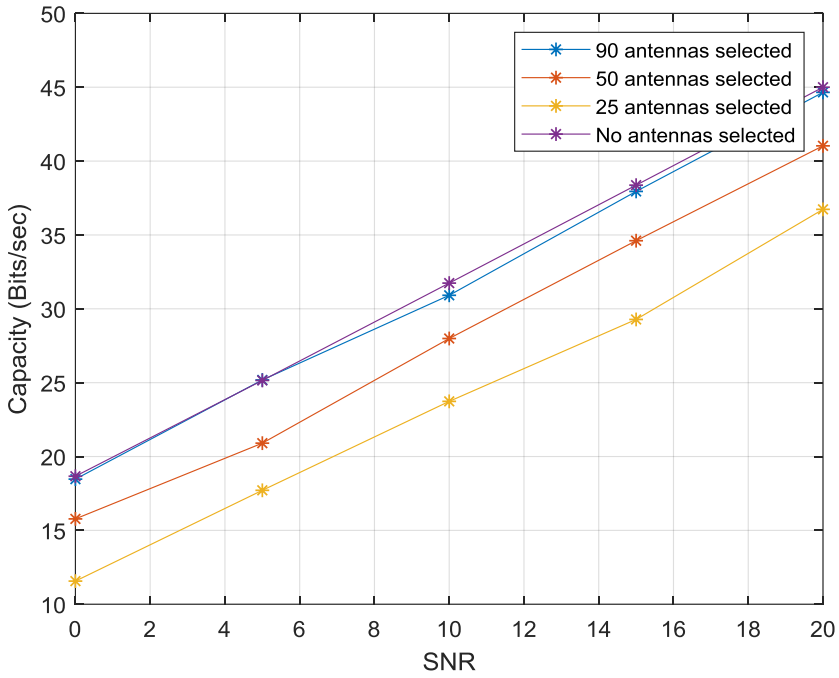

Fig. 2.3. Ergodic Capacity vs. SNR for preselection in massive MIMO (M=100, N given in legend, K=4)

Fig. 2.3 is for a larger (massive) antenna system (M=100; N=90, 50, 25 K=4) and has Suzuki fading (Rayleigh with lognormal, here with a standard deviation of 8dB for the lognormal, with each user having the same lognormal fading for all of the antennas of the massive MIMO). The graph serves to indicate the impact of the proportion of antennas selected in massive MIMO, under a realistic fading channel. The related simulations of [49] do not feature Rayleigh fading, and had an error in the lognormal fading. The increasing presence (i.e., increasing standard deviation) of the lognormal fading, despite being a zero mean change, reduces the capacity, as expected, but the size of the reduction has not been treated before this result. For no lognormal fading (i.e., both mean and standard deviation are zero dB) the capacity is higher by some 5 bits/sec/Hz, essentially independently of the

proportional number of antennas selected. For the preselection, an approximate doubling of the proportion (from 25 to 50 out of 100, and then from 50 to 90 out of 100) also changes this capacity by almost 5 bits/sec/Hz. This is the trade-off between the capacity and a saving in the cost of the RF chains. This trade-off is convenient to manage through the preselection parameters for any such MIMO system, with a range of fading.

2.8 Summary

In this chapter, the problem of antenna subset selection is approximated by a constrained convex relaxation (along with a rounding scheme) that is solved using standard low complexity techniques from optimization theory. Simulation results show that the performance of the scheme is very close to optimal. The use of antenna selection in massive MIMO can reduce the cost of RF chains, with an acceptable capacity loss. Simulation shows that this approach achieves essentially the same performance as the exhaustive search algorithm for antenna selection.

CHAPTER 3: DISTRIBUTED ANTENNAS MIMO CHANNEL SOUNDER

3.1 Overview

Most future wireless links will operate within multipath propagation environments and will use multi-element antennas (MEAs) to suppress interference and maximize capacity. The design of compact, MEAs requires knowledge of the propagation environment because the propagation environment and the embedded element patterns combine to define the channel. While the MEA design is guided by propagation models, the final design should be checked by a physical experiment to ensure appropriate statistical performance, such as low correlations and similar mean gains. Consequently, multi-channel (vector) channel sounding is critical for confirming the operations of compact MEA designs, and even finalizing the design, and to be able to estimate the performance of the associated communication. This chapter describes a technique for the required vector channel sounding using a simple, single-input, single-output channel-sounder. The vector channels are separated by inserting different RoF signal delays into the antenna ports and then combining the antenna signals as a set of separated-in-time responses. The RoF delays must be large relative to the channel delay spreads. In the VNA/channel-sounder, the delayed channels can be easily separated with basic signal processing, ready for statistical analysis.

A promising solution to meet the ever-increasing demand for higher capacity wireless connectivity is basically to deploy smaller cells and use MEAs. The smaller cells mean more re-use of the spectrum. The MEAs allow MIMO communications – the suppression of noise-dominating interference and the use of multiple parallel channels in each link to support higher capacity efficiencies (in bits-per-sec/Hz). In principle, the more antenna elements, the greater the capacity efficiency. The capacity itself can be improved by brute-force techniques such as using extra spectrum, i.e., wide-band systems. There are many terms for these various developments, such as distributed distribution architectures, femto- and pico-cell base-stations/access points deployments, mesh networking solutions, cooperative schemes cognitive radio, and so on. In any event, the multiple, parallel

channels, or vector channels, require certain well-known characteristics for these advanced communications systems to work well. For example, the channels should be uncorrelated, meaning that their narrowband fading envelopes are uncorrelated over time evolution and that the mean channel gains should be similar. For marketable products, the antennas should be physically compact, and their electrical spacing should be minimized. But compactness tends to foster the correlation between the channels. Propagation models are used but at the end of the day, the antennas need to be checked against real-world propagation conditions to ensure the performance of the expected communication. Consequently, the channels need to be sounded in real-world experiments using the same antennas [5] [64] [34]. (The antennas and propagation environment combine to define the channel.) For other aspects of the communications signal processing, other channel parameters are required. For wide-band channels, equalization is required as part of the signal processing, and so knowledge of the delay profile and its modelled parameters such as delay spread, are required for the design of the communications signal processing. All this amounts to the fact that physical channel sounding is still important for developing the new, small-cell links, their communications signal processing, and their compact MEAs.

3.2 Background

Diversity antennas were introduced around the mid-20th century to reduce the narrowband fading envelope fading in communications and sensing systems. The basics for communications were laid out by Stein [4], and applied to mobile communications, including both receive and transmit diversity (later called MIMO) by Jakes [65]. The narrow band signal fades represented dead spots in ubiquitous multipath situations, and the associated channel dispersion at these fades compounded the poor error performance from the reduced signal-to-noise ratio. Spaced, or multiple antennas, offered a solution because the diverse channels faded at different (uncorrelated) times. The required spacing of similar antenna elements (space diversity) was, and still is, typically derived from simplistic propagation models. MEAs, where the elements are not necessarily all the same,

as in an array, offer more degrees of freedom for decorrelating the channels. Because the designs are typically propagation-model-based, physical experiments are needed to verify, or produce a final design, for them. The original works on antenna diversity presented the improvement as an improved distribution for the SNR. Later, the communications literature translated the improved SNR distributions to capacity (or capacity efficiency), in bits/s/Hz, e.g. [66], and this brought greater awareness of the power of multiple antennas to increase link quality to the large information theory and digital communications community.

Since the diversity pioneering days, communications applications have spread quickly. Distributed antennas systems (DAS) – a form of diversity – were introduced simply to cover dead spots in indoor wireless communications [67], and more recent studies [68] have identified other potential advantages. DAS allows capacity gain, coverage improvement, and low power consumption [67] [68] [69] [70] [71]. DAS also reduces inter-cell interference and hence significantly improves performance [72] [73]. FUTON (fiber optic network for distributed, extendible, heterogeneous radio architectures and service provisioning) is a proof-of-concept in Europe for fiber-based distributed antennas technology [72]. Similarly, China's FuTURE project [74] [75] is another example of the implementation of optic fiber based distributed antennas system. From an architectural point-of-view, DAS can reduce the cost of the installing system and simplify maintenance because it reduces a required number of base stations (BSs) within the service area. DAS possess advantages in terms of signal-to-interference-plus-noise ratio (SINR) and capacity due to macro-diversity and reduced access distance.

Even though the quantity of research in MIMO has been remarkable over the past several decades, the theoretic potential of MIMO systems is yet to be realized in practical communications systems. This is partly due to a lack of understanding of characteristics of the channels, particularly in the DAS scenario. Among a large variety of different types of MIMO channel models, the geometry based stochastic approach [76] [77] is mostly used in the literature due to its convenience for simulations of MIMO systems, in particular the spatial and temporal characteristics. But the link between the models and the real-world behaviour is not so easy to tie

down, for compact antenna systems in changing propagation environments, i.e., mobile communications.

Several challenges are associated with the development of distributed channel sounders. There is a large literature, on channel sounders and measurements. Representative, recent examples include [78] [79] [80] [25] [33] [26] [81]. In [80], multilink (MU-MIMO) channel measurements were conducted using a commercially available MEDAV-LUND channel sounder with its corresponding receiver; as well as the receiver from Elektrobit. In [33], the authors consider whether mobile multilink measurements can be emulated by sequentially measuring each point-to-point link, with a single channel sounder. The crucial aspect of this approach is whether it is practically feasible to keep the environment sufficiently static between sequential measurements. Their results indicate that a single channel sounder approach is feasible when the focus is on channel statistics e.g. spatial correlation. When channel matrices are of interest, the approach is limited. An example of state-of-the-art channel sounder and its results are presented in [26], where multilink measurements in an indoor hall environment utilizing a scalable MIMO channel sounder at 11 GHz are presented. The results indicated that eigen-structures of spatially separated links are highly correlated when Rxs share the line-of-sight (LOS) for Tx. Similarly, [26] reviews the advantages of using Universal Software Radio Peripheral (USRP) platform for channel sounding. The motivation for the distributed channel sounder (DCS) becomes necessary to understand the effects of multilink interference. We present a low-cost optic-fiber based scalable DCS, using a standard two-port VSA. The channel sounder uses radio over fiber (RoF) with remote antenna units (RAUs) as distributed nodes to collect data. The nodes are connected to the Zinwave optical hub, which provides a signal combination and switches actions. The ballpark cost of the extra hardware is approximately $23k.

Channel staticness is assumed for a vector channel measurement campaign, due to limitations of channel sounder. Research is currently underway to generalize the existing stochastic and geometric approaches to handle vector channels [82]. This work is motivated by the ongoing high level of interest in distributed antennas,

especially in indoor and short-range vehicular environments, and the fact that channel measurements for DAS are still at an early stage [33], with few researchers focused on low-cost and scalable DCS.

3.3 System Model

The main modules of the DCS are a signal spectrum analyser, fiber-optic cables and MATLAB scripts to control instrument and analyze the data. The spectrum analyzer supports multiple wireless standards, fast data-rate processing and calculates power delay profile (PDP) with high accuracy due to a high sampling rate. The RAUs are connected to a central optical hub, using variable delay lines implemented using RoF cables, to avoid overlapping of the impulse response from individual RAUs. The optic-fiber is better than coaxial cable, because it is more compact, cheaper, and has more linearity. The band is 136-2700MHz. Fig. 3.1 shows the VSA and RAUs used in the DCS. Our approach is simple, i.e. transmit a known PN signal sequence $s(t)$. The received signal $r(t)$ at the VSA is then,

$$r(t) = \int h_1(t,T_1)s^*(t-T_1)dT_1 + \int h_2(t,T_2)s^*(t-T_2)dT_2 + \ldots \quad \textbf{(1)}$$
$$\int h_3(t,T_3)s^*(t-T_3)dT_3 + n(T)$$

where $\int h_1(t,T_1)s^*(t-T_1)dT_1$, $\int h_2(t,T_2)s^*(t-T_2)dT_2$ and $\int h_3(t,T_3)s^*(t-T_3)dT_3$ are the convolutions of transmitted signal and impulse response of the channels RAU-1, RAU-2 and RAU-3 respectively, placed at various locations in an indoor environment. The proposed DCS uses a stepping correlator during MATLAB based processing [83]. We captured the signals received by the three distributed antennas; and pass them through a cross-correlator to recover the simultaneously measured power delay profiles. We used a VSG-based PRBS transmitter to generate the probing signal. Using the VSA gives the luxury of saving frames to a deep memory and then transferring the data to hard disk later, to process the received signals offline.

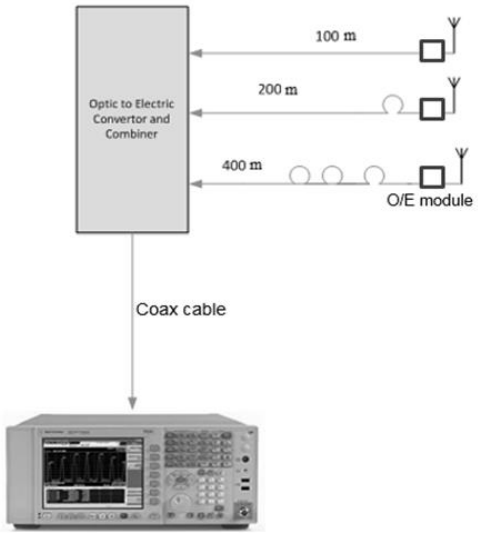

Fig. 3.1. Proposed distributed channel sounder.

3.4 Experimental Setup

3.4.1 System Level Analysis of Scheme

We modulated the PN sequence using VSG signal generator. The generated signal was transmitted from the Tx to three RAUs (multi-nodes) simultaneously. The RAUs work like a distributed receiver connected to the central hub. The RAUs are spaced apart, to make sure there is no inter-link correlation. The raw data is collected using the acquisition module inside the VSA. The VSA collects the received signal and sends it to the PC, where it is stored on the hard-disk for post-processing. We implemented MATLAB based scripts to automate storage, and for data analysis. A separate PC is available, with a graphical user interface (GUI) to let the user interact with the optical hub and manually select RAUs. The configurations of our channel sounder are listed in Table 3.1. We used Agilent PSG to transmit a PN9 PRBS signal with bandwidth between 1 MHz and 80 MHz, in unoccupied bands between 850 MHz and 6 GHz. As listed in Table 3.1, the PN9 sequence comprises of 511 bits, and 1 frame length is 11.3 μs . We transmitted 18 frames of length 205.3 μs and averaged them at the receiver. The data rate (chip-rate) is 44.8 Mbps. For the entire experiment, we kept the transmission power at 25 dBm. On the receiver side, the Nyquist frequency is used for sampling i.e. 2 x

44.8 MHz. This implies that minimum delay that can be measured (delay resolution) is 1/ (2x 44.8 MHz) sec. We used three fiber-optic rolls, each measuring 100 m. Therefore,

$$\text{delay generated by a 100-m roll} = 0.5\,\mu s \qquad \textbf{(2)}$$

Table 3.1. Specifications of DCS.

Quantity	Value
carrier frequency	2300 MHz
System bandwidth	40 MHz
transmit power	20dbm
chip rate	44.4 Mcps
sampling frequency	2x44.4 MHz
code length	511
maximum measurable delay	0.3us
number of transmit antennas	1
number of receive antennas	3
number of measurements	18 frames averaged
delay resolution	1/2x44.4 MHz
capture memory	2 GB
total measurement length	205.3 us
average measurement length	11.3 us
min length of fibers of 3 RAUs	600 m
max length of fibers of 3 RAUs	1100 m
antenna configuration	1x3
RAU antenna type	Omni directional with 4 dBi gain
Polarization	Vertical

3.4.2 Limitations

One of the limitations of proposed DCS is that noise level increases during correlation if more signals are combined at the combiner. Secondly, the number of antennas supported by this system is limited by the total delay line. Thirdly, the RAUs must be separated no less than average CIR i.e., signal strength and channel must be differently experienced at each antenna. Fourth, in this experiment, we have assumed a single transmitter and three RAUs. We can extend this approach, to a multiuser environment by using another VSG with an

orthogonal PN sequence. The orthogonal PN sequences can be easily de-correlated at the VSA.

3.5 Experimental Setup

To test the proposed DCS, we carried out an indoor experiment in a corridor environment. This was a typical P2MP (point to multipoint) experiment configuration. We assumed that both Tx and Rx are static. The RoF delay for RAU 1, RAU 2 and RAU 3 are 0.3 μs , 0.6 μs and 0.9 μs respectively. The three fiber units are combined at the central optical hub. We analyzed and plotted the results using MATLAB. Fig 3.2 gives the overlaid power delay profile over a 10-time length. We have kept the transmit power low as 20 dBm. The floor level in the PDP is -42 dBm. Fig 3.3 gives the averaged power delay profile for a 10-time length. The presence of three distant correlation peaks corresponding to the three PDPs is visible in the plot. Fig. 3.6 shows the gear of proposed DCS. Fig. 3.6(a) is the transmit planar antenna; Fig 3.6(b) is the Zinwave optical hub, fitted with optical-to-electric converters on the front, and a GigE Ethernet cable connected to a laptop for manual configuration. Fig. 3.6(c) is the RAU laying on the table and connected to a vertical antenna. This antenna can transmit and receive, though we used it for the reception. Fig. 3.6(d) shows the VSA, mounted on a cart with an external laptop, with MATLAB scripts for post-processing.

Index of refraction of fibre is 1.4682 at 1550nm, and speed of light through fibre=204190477 m/s, which is not the same as speed of light though space. We calculate the corresponding time took for the light waves to traverse the fiber optics of different lengths, i.e.

100m/204190477m/s=0.5us
200m/204190477m/s=1us
400m/204190477m/s=2us

Table 3.2. RAUs and their corresponding optical delays.

RAU	Optic fiber delay
2	0.5 μs
1	1 μs
3	2 us

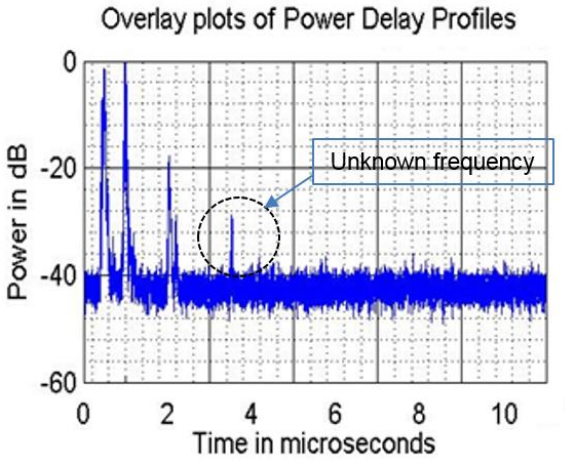

Fig. 3.2 Overlay plots of power delay profile.

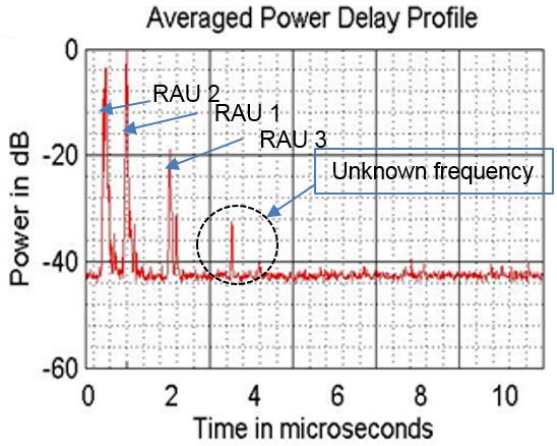

Fig. 3.3. Averaged power delay profile.

3.6 Summary

Vector channel-sounding is an expensive task, traditionally because each channel requires its own VNA ports. If the multiple channels can be separated in time, then

a standard two-port measurement will suffice for vector channel sounding. Such a technique is to interleave all the different channels by delaying them by different amounts and use basic signal processing to separate the channels for subsequent statistical processing. The use of optic fiber delays has been presented, along with the results from physical measurements of a demonstration system. The extra equipment required is the optical fibers, their interconnections between the antennas and the VNA, and the signal combination is relatively inexpensive relative to a multiport VNA.

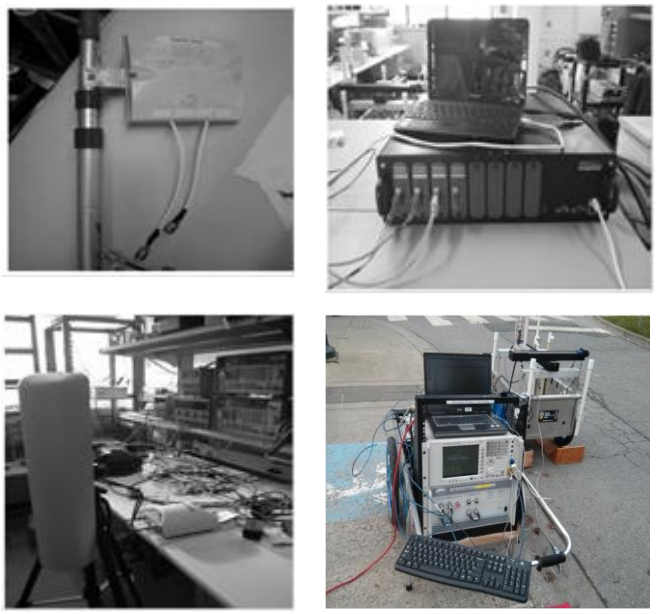

Fig. 3.4. Measurement gear for DCS, (a) transmit antenna (b) optic-fiber combiner and hub (c) remote antenna unit (RAU) (d) VSA with a laptop for post-processing

CHAPTER 4: FIBER-FED DISTRIBUTED ANTENNA SYSTEM IN AN FPGA SOFTWARE DEFINED RADIO FOR 5G DEMONSTRATION

4.1 Overview

In this chapter, we describe the implementation of STBC-OFDM on Virtex-6 software defined radio (SDR) with experimental measurements. The implementation of high-speed 4G LTE and FuTURE wireless network in a real-time environment demands ever-increasing hardware processing capability. The field programmable gate array (FPGA) has the potential to solve this problem since it provides reconfigurable logic with high parallelism and low-power solutions, unlike other alternatives e.g. DSP processors, ASIC and general-purpose processor in the market. Our STBC-OFDM design makes use of DSP48E slices for computationally intensive mathematical routines and Xilinx Microblaze soft-processors for real-time data exchange (RTDX) with the host computer. Our design works in the ISM band and supports a system bandwidth of 20 MHz. We present a high-level Xilinx System Generator design of physical layer algorithms for STBC-OFDM. For real-time implementation, the receiver is equipped with time-offset synchronization and frequency-offset estimation modules. In this chapter, real-time indoor measurements are performed in the 2.5 GHz ISM-band. Our MIMO test-bed consists of a modular hardware platform consisting of SDR and radio front-end transceiver modules. The centralized SDR test-bed allows options for both real-time and offline baseband processing. The FPGA resources consumed on FPGA during real-time MIMO-OFDM implementation are presented. Some measurement results are presented. In this work, we present in detail the implementation of a real-time SDR-based 2×2 STBC-OFDM system that

constitutes the cornerstone of our efforts to achieve a powerful, reconfigurable, and modular fiber based DAS test bed.

4.2 Background

As the future broadband wireless communication systems are constantly expected to provide ever higher communication data-rates (~1Gbps for low mobility users and 300 Mbps for mobile terminals). It has already been well established [3] [64] [84] that multiple-input multiple output (MIMO) scheme can provide this high data-rate demand since MIMO can increase link capacity using additional spatial degree-of-freedom. MIMO also provides benefits like extended coverage, reduced interference, and reliable communication by using advanced smart antennas features such as spatial multiplexing, space-time block coding (STBC) and beamforming. Combined with OFDM modulation, MIMO is the enabler of modern wireless broadband communication techniques. The broadband communication owes to the OFDM, which has the ability to cope with severe frequency-selective multipath channels by converting the broadband channel into a series of parallel orthogonal sub-channels with a bandwidth smaller than the channel's coherence bandwidth, thereby ingeniously reducing the effects of inter-symbol interference. Recently, MIMO-OFDM has also been extended to fiber connected distributed antennas architectures; as a promising technique to meet the ever increasing demand for the wireless connectivity [71] [85] [86]. The massive parallelism and pipelining required for intensive baseband signal processing in a real-time MIMO-OFDM test-bed makes FPGA platforms appropriate candidate for implementing next-generation broadband fiber connected DAS. This means that FPGA based

signal processing systems are becoming a practical choice for the researchers and engineers to attain 4G capacity criteria. Consequent with this new direction, this chapter implements the physical layer design of an STBC-OFDM transceiver on a software defined radio (SDR) equipped with Virtex-6 FPGA and high-speed ADCs/DACs. The focus of our effort is to fill the gap in the literature regarding the presence of experimental demonstration and challenges involved for implementing the MIMO-OFDM technology on FPGA.

4.3 System Model

The STBC-OFDM system is equipped with two to transmit and receive antennas. The system operates in a frequency-selective Rayleigh fading indoor environment. The system assumes a quasi-static channel (i.e. the channel is assumed to be constant during the packet duration). We have used the multipath MIMO channel model as described in [19]. Suppose that the channel impulse response can be approximately recorded with L time-instances, then the fading-channel between p^{th} transmitter and q^{th} receiver antennas can be modelled by a discrete baseband $(M-1)^{th}$ order FIR-filter; with filter taps $g_{qp}(l)$ where $l=\{0,\ldots,M-1\}$. The taps are assumed i.i.d zero-mean complex Gaussian random variables with a variance $\frac{1}{2}P(l)$ per dimension. Suppose that $g_{qp}(l)$ is the $(q,p)^{th}$ element of the matrix $G(l)$, then the discrete-time MIMO baseband signal model is given by [19],

$$r(\tau)=\sum_{l=0}^{M-1}G(l)u(\tau-l)+v(\tau) \tag{1}$$

We used the orthogonal frequency division multiplexing (OFDM) as a downlink transmission scheme. OFDM is a block modulation technique, where a block of N symbols is transmitted in parallel using N sub-carriers. The time duration of an

OFDM symbol is N times larger than that of a single-carrier system. OFDM modulation is implemented as an inverse discrete Fourier transform (IDFT) on a block of N symbols. To mitigate the effects of inter-symbol interference (ISI) caused by the channel time-spread, each block of N IDFT coefficients is preceded by a cyclic prefix (CP) or a guard interval consisting of G samples, such that the length of the CP is at least equal to the channel. OFDM is an effective strategy for dealing with frequency-selective channels [45] [87]. When the sub-channel bandwidth is sufficiently narrow, the frequency response across each sub-channel is approximately flat avoiding the need for complicated time-domain equalization. These flat-fading sub-channels provide an effective platform on which space-time algorithms developed for a flat-fading channel can be applied.

4.4 Transmitter Model in VLSI

The 20MHz baseband transmitter requires a high bandwidth of SDR [88]. The fully pipelined Xilinx FIR IP cores are utilized to accomplish the wideband FIR filters at the baseband level. The transmitter operates in packet mode with a preamble of four symbols. The initial two OFDM symbols are dedicated to blocking boundary detection and coarse carrier frequency offset (CFO) estimation [89]. The following two OFDM symbols are used in 2×2 MIMO channel matrix estimation. Continuous pilots are embedded at specific subcarriers for CFO tracking, as well as to estimate and correct phase noise [90]. The overall packet length is maintained shorter than the coherence time of the channel.

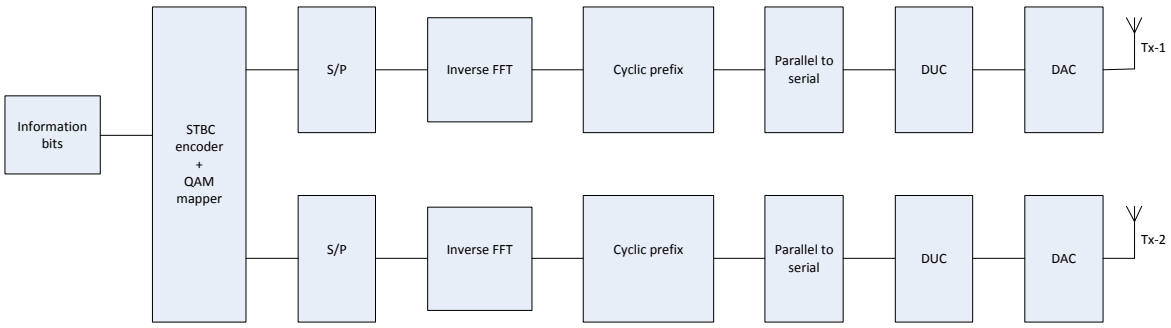

Fig. 4.1. Block diagram of the transmitter.

The block diagram of the transmitter is shown in Figure 1. We briefly describe it as follows. The QPSK modulator maps the bits coming from scrambler to constellation-points, and the subcarrier mapper allocates the symbols to corresponding subcarriers [20] [91]. The MIMO algorithms are then applied on per OFDM subcarrier basis and are like single carrier algorithms. The FFT encodes the block frame for OFDM transmission. We have used the Xilinx FFT IP-core that implements a computationally efficient method for calculating DFT. The core provides an optional cyclic prefix insertion for digital communications systems and can compute the FFT up to 2048 points. The cyclic prefix serves two purposes, 1−as guard interval; it eliminates the inter-symbol interference from the previous symbol, and 2−As a repetition of end of the symbol, it allows the linear convolution of a frequency selective multipath channel to be modelled as circular convolution, which in turn may be transformed to the frequency domain using DFT [21] [92] [93]. This approach allows for simple frequency-domain processing such as channel estimation and equalization. The baseband signal is then upconverted to an intermediate frequency (IF). Utilizing an IF avoids the problems of DC offset, carrier leakage, I/Q imbalance [91]. The DUC, as shown in Figure 2, translates one

or more channels of data from baseband to passband. It achieves this operation using interpolation to increase the sampling rate, filtering to provide the spectral shaping and rejection of the interpolation images, and mixing to shift the signal spectrum to the desired carrier frequency.

To encode the data, we use the Alamouti space-time block coding (STBC) technique [85]. STBC improves signal quality at the receiver by means of simple processing across two transmit antennas, without any feedback from the receiver. The diversity order obtained equals to the maximal-ratio combining receiver. STBC requires no bandwidth expansion, as redundancy is applied in space across multiple antennas. At a given symbol period, two signals are simultaneously transmitted from the two antennas. STBC is applied to MIMO-OFDM by regarding each sub-channel as a virtual antenna [93] [94] [95]. STBC-OFDM can then exploit space diversity; however, the potential multipath diversity offered by multipath is not used. As mentioned before, OFDM converts a wideband channel into parallel narrowband sub-channels. OFDM enables STBC in real life. In STBC-OFDM, time index used in STBC is replaced by the tone index of OFDM. Also, since STBC requires a channel to remain constant over consecutive symbol periods in STBC-OFDM context, the channel must remain constant over consecutive tones. The implemented STBC-OFDM transmitter using MATLAB and Xilinx System Generator is shown in Figure 3.

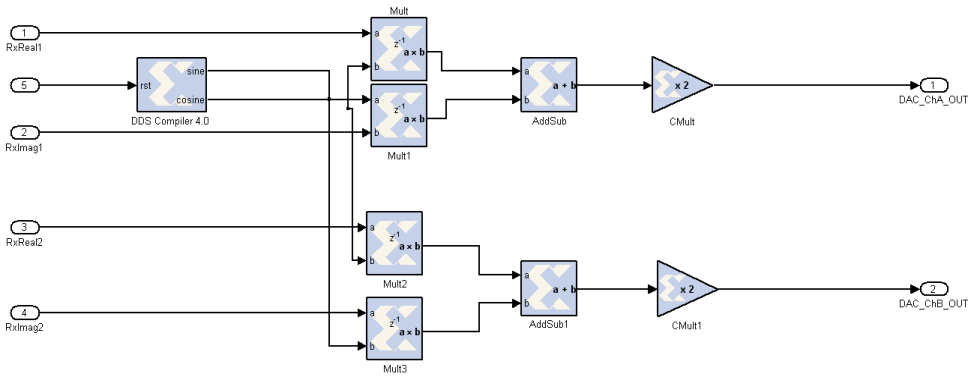

Fig. 4.2. DUC model for Virtex-6 FPGA.

Table 4.1: Encoding and transmission sequence for STBC-OFDM.

	subcarrier k	***subcarrier k+1***
A	s_1	s_2
B	s_1	$-s_2^*$
C	s_2	s_1^*

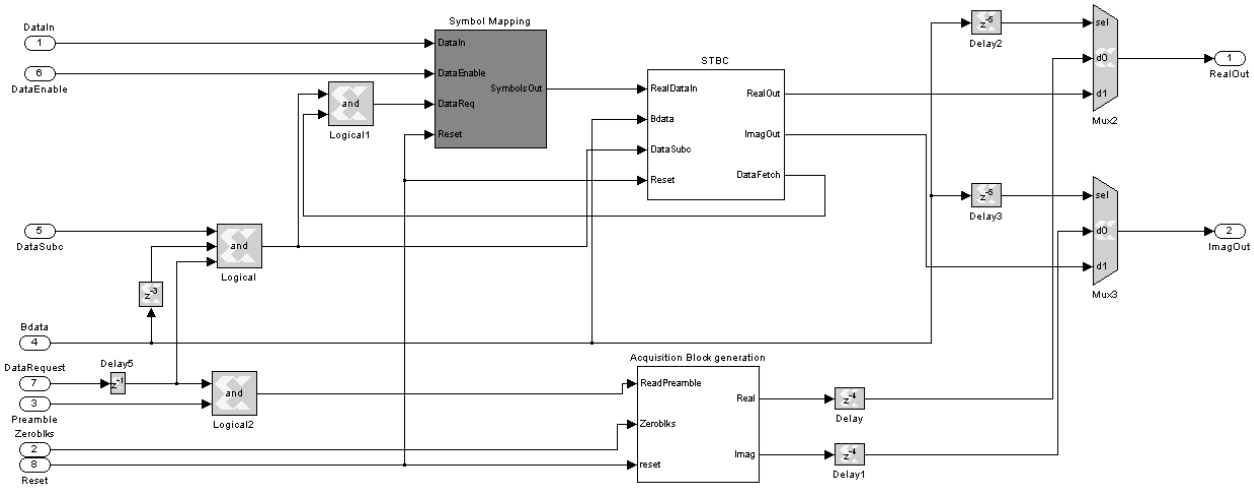

Fig. 4.3. Model of STBC module for Virtex-6 FPGA.

Figure 4 describes how the STBC scheme is applied to the multi-carrier system followed by Table 1. Figure 5 shows the BER vs. SNR plot to confirm the idea that 2×2 STBC-OFDM provides the same diversity order as 4×1 MRC. The OFDM for

the single transmitter and receiver link is also shown for comparison. Figure 6 gives a Xilinx System Generator model for STBC-OFDM transmitter. The model includes packet and encoding module, pilot insertion and data loading block, FFT and cyclic prefix blocks, etc [96].

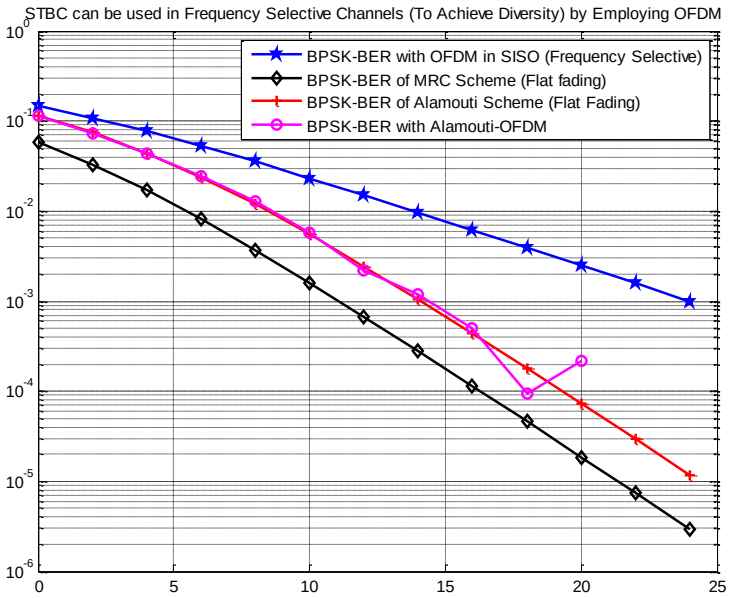

Fig. 4.4. Performance comparison for MIMO-OFDM, OFDM, and MRC over frequency selective Rayleigh block-fading channel.

4.5 Receiver Model in VLSI

The block diagram of the receiver is shown in Figure 7.The main modules of STBC-OFDM receiver, 1. Digital down conversion, 2. carrier frequency offset estimation, 3. channel estimation and equalization and 4. STBC-OFDM decoder.

4.5.1 Digital down converter

The digital down converter (DDC) down-converts the intermediate frequency (IF) signal to digital baseband. The digital down converter (DDC) implements three

functions namely, channel frequency translation, I/Q components extraction, and signal decimation. Finally, an output decimator delivers the complex representation of the digitized signal [96].

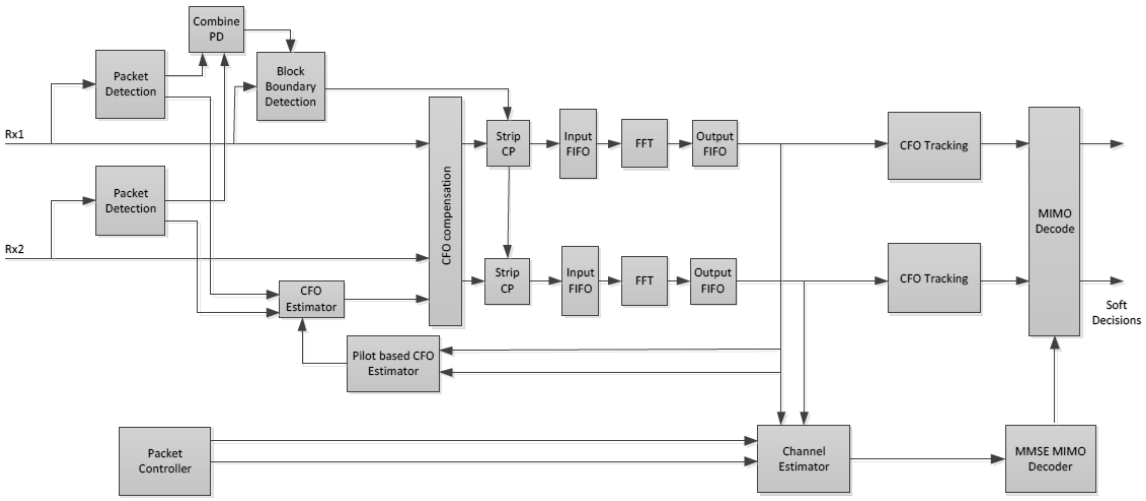

Fig. 4.5. Block diagram of the receiver

4.5.2 Frame synchronization

Wireless communication usually occurs in packets (i.e. series of short bursts). A key requirement for MIMO transmission involves the detection of transmitted bursts and timing and frequency synchronization [88]. Receivers generally synchronize by calculating the autocorrelation function of the preamble placed at the beginning of the signal. We have implemented the Schmidl and Cox algorithm [89] [94] for estimating the joint time-offset and frequency synchronization. This algorithm uses the delay correlation approach as it involves providing two identical preamble frames. The frame synchronization first detects the beginning of the data period, and accordingly the position of the OFDM symbol to apply the FFT.

Second, it estimates CFO that will be used to finely tune the DDS described in section 4.1. The frequency offset is caused by the difference in oscillator frequencies at transmitter and receiver. The carrier frequency offset tracking needs scattered pilots to estimate the CFO. The amount of angular rotation from one OFDM block to the next is proportional to the CFO. Figure 9 shows the System Generator model for timing offset and frequency synchronization blocks. Figure 10 shows a theoretical BER vs. SNR plot for various frequency offsets. It is concluded that if CFO is larger than a few subcarriers, the receiver will not be able to demodulate the signal properly.

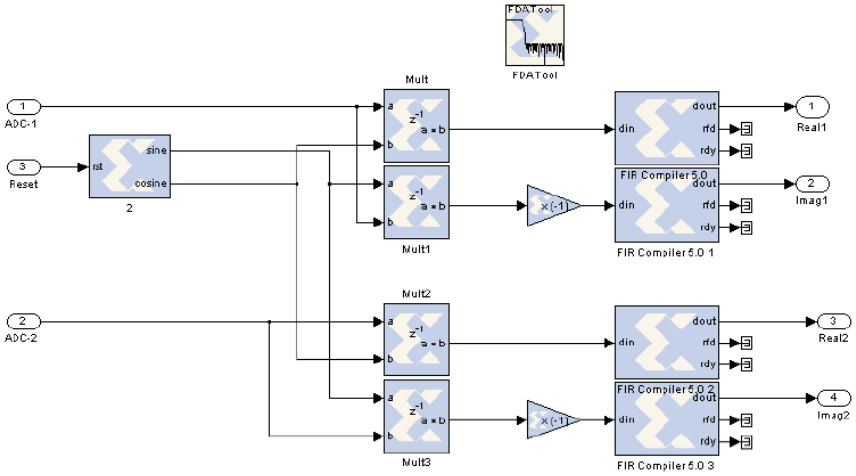

Fig. 4.6. DDC model for Virtex-6 FPGA.

The timing metric $M(d)$ for this module is expressed [25] by Equation (2). $P(d)$ determines the correlation of the signal. The timing metric is normalized by the maximum power received in the signal.

$$M(d) = \frac{|P(d)|^2}{(R(d))^2}$$

$$P(d) = \sum_{m=0}^{L-1} \left(r_{d+m}^{*} r_{d+m+L} \right) \quad \text{– Delay correlation} \qquad (2)$$

$$R(d) = \sum_{m=0}^{L-1} |r_{d+m+L}|^2 \quad \text{– Received power}$$

4.5.3 Channel Estimation

We describe briefly the channel estimation process that was implemented inside the receiver. We used a pilot-aided channel estimation process that uses the least-squares method to estimate the channel [97]. We implemented the algorithm using the C++ algorithm embedded inside the Microblaze processor and interfaced it with our remaining System Generator design. Before discussing the MIMO channel estimation process, let us first describe SISO-OFDM channel estimation. We modified that algorithm for the multiple antennas scenarios. MIMO-OFDM channel estimation works on the same underlined procedure. In the SISO-OFDM system, data is transmitted in frames of N tones each, with additional P tones added for cyclic prefixing [98].

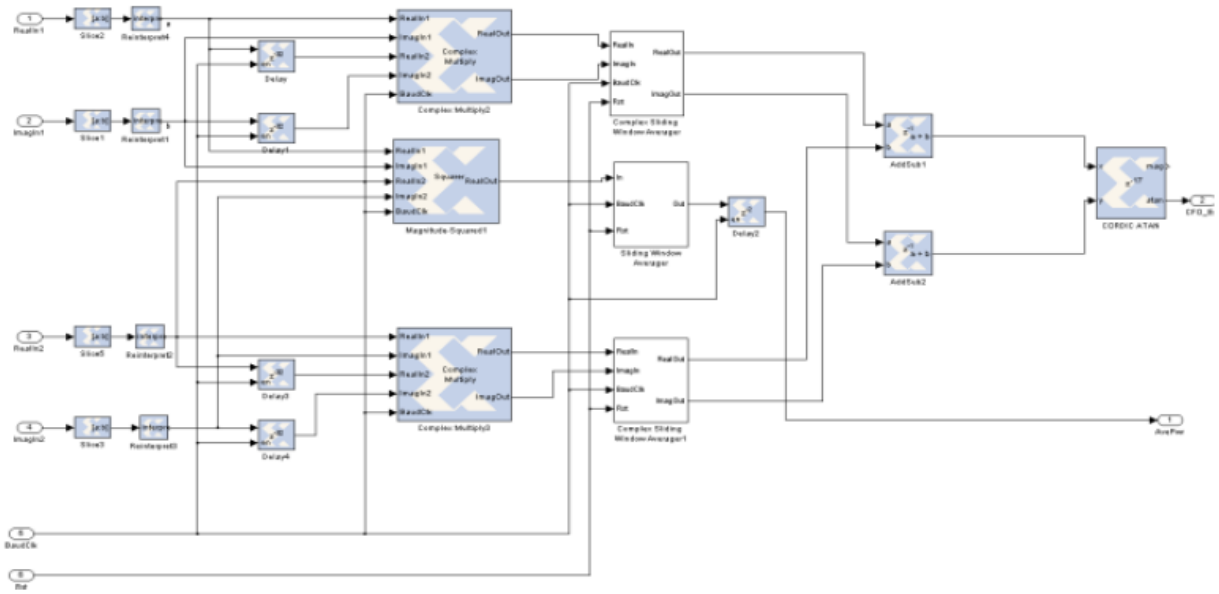

Fig. 4.7. Model of coarse CFO estimation and block boundary detection module.

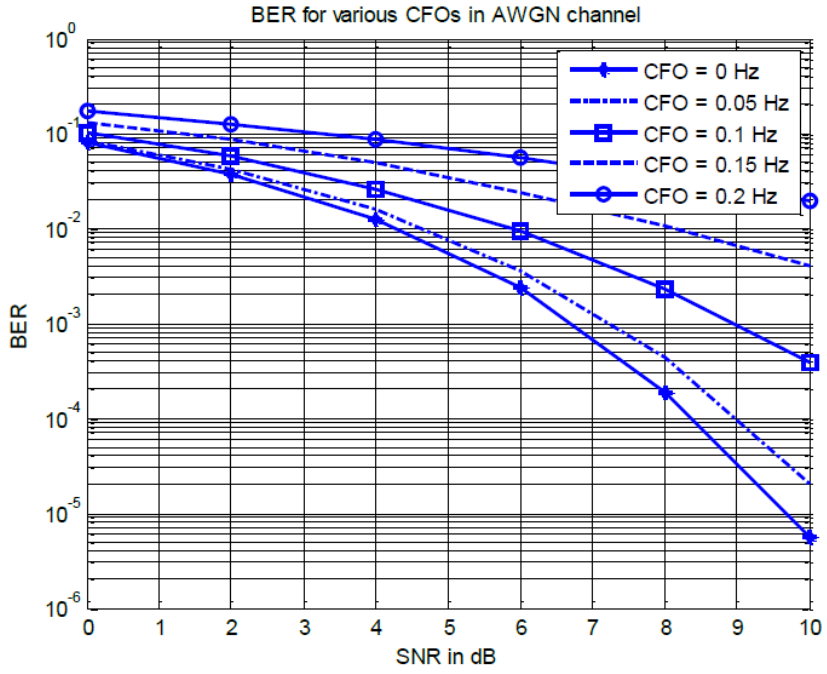

Fig. 4.10. BER increases with varying frequency offset.

There are various channel estimation algorithms for MIMO available in the

literature. We used the frequency domain channel estimation technique, and least-squares to estimate the channel. Before discussing the process of MIMO channel estimation, we first describe the SISO-OFDM channel estimation. In an OFDM system, the data are transmitted in blocks, say of size N tones each, with additional P tones added for the cyclic prefixing purposes [99]. Specifically, consider a block of data of size N,

$$s = col\{s(N-1), s(N-2), \ldots, s(0)\} \tag{4}$$

Before transmission, this block of data is transformed by the inverse DFT matrix i.e. s is transformed in to $\bar{s} = F^* s$, where F is a unitary DFT matrix of size N defined by,

$$\lfloor F \rfloor_{ik} = \frac{1}{\sqrt{N}} e^{\frac{-j2\pi ik}{N}} \tag{5}$$

Then the cyclic prefix of length P is added to the transformed data so that the transmitted sequence ends up being,

$$col\left\{\underbrace{\bar{s}(N-1), \bar{s}(N-2), \ldots, \bar{s}(0)}_{\text{transformed block of size } N}, \underbrace{\bar{s}(N-1), \bar{s}(N-2), \ldots, \bar{s}(N-P)}_{\text{cyclic prefix of size } P}\right\} \tag{6}$$

with the rightmost sample transmitted at time instant 1, and the leftmost sample transmitted at a time instant $N+P$. At the receiver, these $(N+P)$ samples are observed in the presence of the additive noise and collected into vector,

$$col\left\{\underbrace{\bar{y}(N+P-1), \bar{y}(N+P-2), \ldots, \bar{y}(P)}_{\text{last N received samples}}, \underbrace{\bar{y}(P-1), \ldots, \bar{y}(2), \bar{y}(1), \bar{y}(0)}_{\text{first P received samples}}\right\} \tag{7}$$

The first P received samples are discarded, while the remaining N received samples are collected into a $N \times 1$ vector $\bar{y}$. To recover the transmitted signals, the channel taps are needed (i.e. Λ is needed). Different training schemes can be used to enable the receiver to estimate the channel, and consequently Λ. The most

common training scheme is to allocate some of the tones i.e., some of the $\{s(i)\}$ in an OFDM symbol, to the known training data. The channel taps are then estimated as described in [87]. Assuming an M -tap FIR model for the channel with impulse response sequence,

$$h = col\{h(0), h(1), \ldots, h(M-1)\} \tag{8}$$

The transform-domain equation of received signal as follows,

$$\bar{y} = H\bar{s} + \bar{v} \tag{9}$$

where H is the channel Toeplitz matrix and $\bar{v}$ denotes the measurement noise in the transformed domain. Since H has a circulant structure, it can be diagonalized by the DFT matrix. Let $\Lambda = FHF^*$ be the diagonalized channel, and multiply the above equation by F from the left. Then the time-domain signal we obtain is,

$$y = \Lambda s + v \tag{10}$$

where time-domain vector quantities $\{y, s, v\}$ are defined by,

$$y = F\bar{y},\ y = F\bar{s},\ v = F\bar{v} \tag{11}$$

If λ be a column-vector with entries of Λ i.e. $\lambda = diag\{\Lambda\}$. Then,

$$\lambda = F^* \begin{bmatrix} h_{M\times 1} \\ 0_{(N-M)\times 1} \end{bmatrix} \tag{12}$$

i.e. λ is the inverse DFT of channel impulse response with its length extended to N. To recover the transmitted signal, the channel taps are needed (i.e. Λ is needed). Different training schemes can be used to enable the receiver to estimate the channel, and consequently Λ. The most common training scheme is to allocate

some of the tones in an OFDM symbol to known training data. The channel taps are then estimated as follows. The system model $y = \Lambda s + v$ can be rewritten as follows,

$$y = \begin{bmatrix} s(N-1) & & & \\ & s(N-2) & & \\ & & \ddots & \\ & & & s(0) \end{bmatrix} \lambda + v \triangleq S\lambda + v \tag{13}$$

Let $\{k_1, k_2, \cdots k_L\}$ denote the indices of $L(L \geq M)$ elements of s that are used as training tones and are therefore known. We collect these transmitted training tones which are also known and hence deterministic quantities and the corresponding received data into two vectors.

$$s_t = col\{s(k_L), s(k_{L-1}), \ldots, s(k_1)\} \tag{14}$$

$$y_t = col\{y(k_L + P), y(k_{L-1} + P), \ldots, y(k_1 + P)\} \tag{15}$$

Let Q denote a $M \times L$ submatrix of F i.e.

$$Q_{M \times L} = \begin{bmatrix} [F]_{0,k_1} & [F]_{0,k_2} & \cdots & [F]_{0,k_L} \\ [F]_{1,k_1} & [F]_{1,k_2} & \cdots & [F]_{1,k_L} \\ \vdots & & \ddots & \vdots \\ [F]_{M-1,k_1} & [F]_{M-1,k_2} & \cdots & [F]_{M-1,k_L} \end{bmatrix} \tag{16}$$

and let S_t be the corresponding $L \times L$ sub-matrix of S i.e. $S_t = diag\{s_t\}$. Then,

$$y_t = \underset{L\times M}{S_t Q^*}\ \underset{M\times 1}{h} + v_t \tag{17}$$

where v_t is corresponding noise vector, $v_t = col\left\{v(k_L+P), v(k_{L-1}+P), \ldots, v(k_1+P)\right\}$. We can now recover h by solving the least-squares problem as [100],

$$\hat{h} = \left[QS_t^* S_t Q^*\right]^{-1} QS_t^* y_t \tag{18}$$

As S_t is diagonal, and assuming that the training data satisfy $|s(i)|^2 = 1$; so $S_t^* S_t = I$, then the above least-squares expression simplifies to,

$$\hat{h} = \left[QQ^*\right]^{-1} Q \begin{bmatrix} y(k_L+P) \big/ s_t(k_L) \\ \vdots \\ y(k_2+P) \big/ s_t(k_2) \\ y(k_1+P) \big/ s_t(k_1) \end{bmatrix} \tag{19}$$

The estimation of Λ is, therefore.

$$\hat{\Lambda} = diag\left(\hat{\lambda}\right) = diag\left(F^* \begin{bmatrix} \hat{h} \\ 0 \end{bmatrix}\right) \tag{20}$$

In order to extend the above procedure to the STBC-OFDM, the training-pattern is coded across dimensions other than frequency e.g. time (OFDM symbols) and space (transmit antennas). The orthogonal training sequence is usually assigned to each antenna individually. Afterward the same training sequence is used for each subcarrier transmitted from its respective antenna. At the receiver, orthogonality of the training sequences is used to distinguish between various antennas and use the channel estimation procedure.

4.5.4 STBC-OFDM decoder

Once the channel is estimated, the STBC-OFDM symbols can be recovered. The received OFDM symbols in two time-intervals are given as [101],

$$\begin{bmatrix} Y_{00} & Y_{01} \\ Y_{10} & Y_{11} \end{bmatrix} = \begin{bmatrix} \Lambda_{00} & \Lambda_{01} \\ \Lambda_{10} & \Lambda_{11} \end{bmatrix} \begin{bmatrix} X_0 & -X_1^* \\ X_1 & X_0^* \end{bmatrix} + \begin{bmatrix} Z_{00} & Z_{01} \\ Z_{10} & Z_{11} \end{bmatrix} \tag{21}$$

where $\Lambda_{00}, \Lambda_{01}, \Lambda_{10}$ and Λ_{11} are diagonal matrices whose elements are DFTs of respective channel impulse-responses h_{00}, h_{01}, h_{10} and h_{11}. Assuming channel estimates available at receiver; then least-square estimator gives the transmitted OFDM symbols,

$$\begin{bmatrix} \hat{X}_0 \\ \hat{X}_1 \end{bmatrix} = \frac{1}{\left|\hat{\Lambda}_{00}\right|^2 + \left|\hat{\Lambda}_{11}\right|^2} \begin{bmatrix} \hat{\Lambda}_{00}^* & \hat{\Lambda}_{01} \\ \hat{\Lambda}_{10}^* & -\hat{\Lambda}_{11} \end{bmatrix} \begin{bmatrix} Y_{00} & Y_{01} \\ Y_{10} & Y_{11} \end{bmatrix} \tag{22}$$

Figure 11 gives a Xilinx System Generator model of the Alamouti matrix computation inside the hardware.

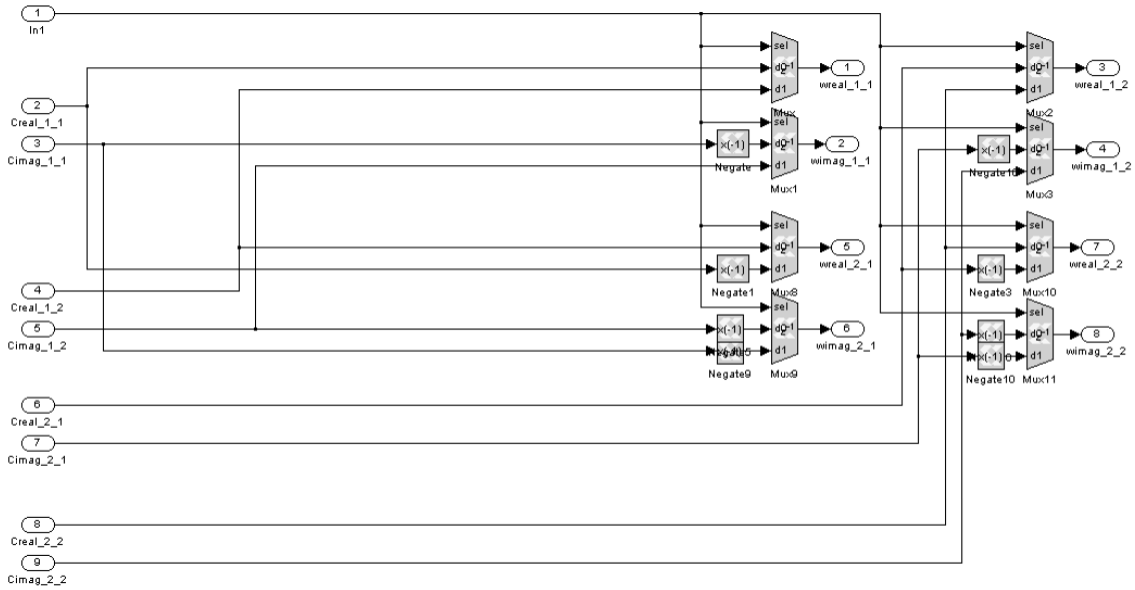

Fig. 4.9. Model of weight matrix computation module.

4.6 Real-Time MIMO Implementation

A real-time STBC MIMO-OFDM system is built, to verify the working of MIMO in the real propagation environment. The STBC-OFDM system operates in the 2.5 GHz ISM band and transmits a broadband signal with 20 MHz bandwidth. Most of the previous implementation approaches that enable rapid prototyping are based on offline signal processing. These offline methods lack insights in implementation complexity and limitations that characterize a real-time MIMO-OFDM system. Also, offline MIMO systems are not suitable to implement adaptive real-time systems for high-speed MIMO networks.

4.6.1 Software-defined radio technology

Software-defined radio (SDR) devices include both software and hardware that can be dynamically reconfigured to enable communication between a wide variety of changing communications standards, protocols, and radio links. The main concept behind the SDR is that different transceiver functions are executed as software programs running on suitable processors (e.g. DSP boards, FPGAs, GPUs). The SDR platform guarantees full compatibility among different wireless technologies. The use of SDR enables wireless communication system to configure itself to multiple wireless standards without changing the hardware. Various MIMO test-beds based on SDRs are available for implementation of novel signal processing algorithms. A typical software defined radio hardware test-bed includes hardware components e.g., RF frontend, baseband components and software development tools [102]. While theoretical results show the performance gains of MIMO wireless communication under idealistic assumptions, a suitable hardware implementation is necessary for validating these gains in a realistic scenario. The leading SDR manufacturers are Nallatech, Lyrtech, Sundance, ICS, Ettus Research and Beecube. The commonly used software development tools are Mathworks tool-suite, Code Composer Studio (CCS), and FPGA programming tools like Xilinx ISE, Xilinx System Generator and Altera DSP Builder. MIMO platforms at various research institutes include GEDOMIS, TU-WIEN, WARP,

UCLA, UCLA2, Montreal, BEECUBE, Wind-Flex MIMO, etc. The RF front-end is the most distinguishing property amongst the mentioned MIMO test beds. The frontends of most MIMO platforms work in the ISM bands (2.4 GHz or 5 GHz). GEDOMIS uses Lyrtech hardware platform and can operate in both bands. The UCLA test bed works on the 5 GHz frequency band, while UCLA2 works on 2.4 GHz band. TUWIEN and WARP work in the 2.4 GHz band. The bandwidths of the RF frontends vary from less than 5 MHz to 40 MHz. The MIMO SDRs can also be distinguished based on their processing capability. The real-time signal processing in SDR platforms is usually carried out using a combination of FPGAs, DSPs or both. The following SDRs do not contain the DSP processor in their platform, e.g. WARP, Lyrtech Perseus, UCLA, TU-WIEN. The remaining SDRs use either a Texas Instruments fixed-point DSP processor e.g., C62xx, C64xx or a floating point C67xx DSP processor. Regarding the FPGAs, most SDRs use Xilinx's Virtex or Spartan series. The MIMO SDRs are also equipped with onboard RAM for storing and processing signals. Table 4 gives a comparison of the technical features of various test-beds. The availability of high-speed signal processing on SDR will allow the implementation of new signal processing techniques at a reduced cost.

Table 4.2. Summary of technical features of current MIMO test-beds.

	GEDOMIS	TUWIEN	UCLA	UCLA2	Montreal	Rice WARP	BEECUBE	UBC
Tx × Rx	4×4	4×4	1×1	4×4	4×4	2×2	–	2×2
Carrier	VME	PCI	PCI	VME	RAID PCI	PCI/USB	PCI	uTCA
Baseband	PC/DSP/FPGA	PC/DSP/FPGA	PC	PC/DSP/FPGA	PC	FPGA	FPGA	FPGA/DSP
DSP	4×C6203	2×C6416	–	4×C6701	–	–	—	C6455
FPGA	6×Spartan II 2x Virtex II	2×Virtex II	–	2× Virtex II	6× Virtex II	–	SXT 315/475	Virtex 6 SXT 475
Buffers	–	Yes	Yes	Yes	Yes	–	Yes	Yes
DAC	16 bit, 320 MHz	14bit, 200 MSPS	16 bit, 100 MHz	12 bit/ 200 MHz	14 bit/ 65 MSPS	–	12bit/ 5GSPS	16bit/ 1 GSPS
ADC	12 bit, 80MHz	14 bit, 100 MSPS	14 bit, 50 Mhz	12 bit/ 105 MHz	12 bit/ 65 MSPS	–	10bit/5GSPS	14bit/ 250MSPS
BW 2.4 GHz	40 MHz	20 MHz	–	20 MHz	3.5 MHz	20 MHz	–	80 MHz
BW 5 GHz	40 MHz	–	25 MHz	–	–	–	–	80MHz

4.6.2 STBC-OFDM broadband test-bed architecture

We present salient features of STBC-OFDM testbed. Figure 12 shows our system architecture.

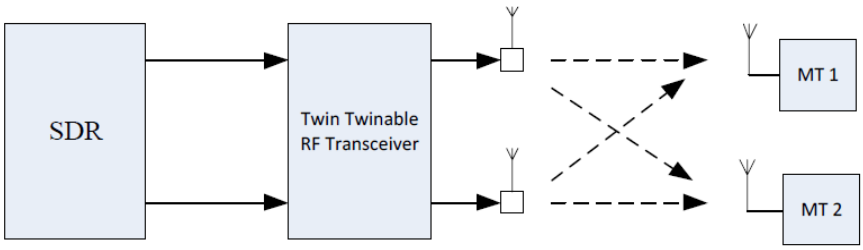

Fig. 4.10. The system architecture of testbed.

The Lyrtech SDR contains the powerful Virtex-6 FPGA. It has support for modular add-on FMC-based I/O cards. The Virtex- 6 FPGA offers a tradeoff between high-performance logic and massive digital signal processing power. Figures 13 shows the Perseus SDR that can be directly inserted in the µTCA chassis; while Figure 14 shows the peripheral blocks on the Perseus SDR.

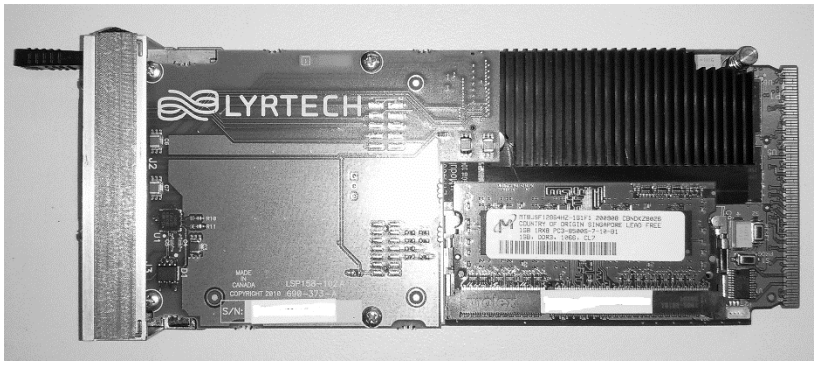

Fig. 4.11. software defined radio [102].

To design a sophisticated real-time system like STBC-OFDM on FPGA device requires handling multiple technical issues, from setting-up, configuring and calibrating the system to successfully validating the entire low-level design. We followed an iterative development-flow throughout the process. Simulations were carried out for various transceiver algorithms in the MATLAB environment. Afterward, the SIMULINK environment was used to architect the model-based design flow. Successful synthesis and place-and-route were performed to proceed with testing and verification in the indoor lab environment. We performed debugging of the FPGA design using Xilinx Chipscope.

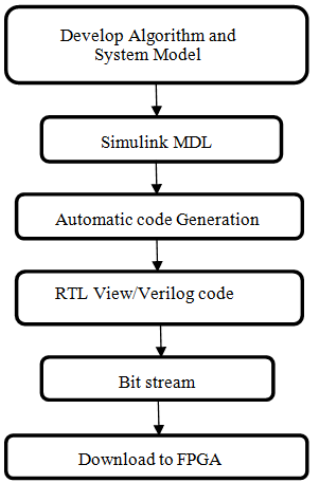

Fig. 4.12. Software integration in SDR.

We used the WiMAX ISM band RF transceiver in our experiments.

4.7 Experimental Measurements

We setup an indoor laboratory measurement of the developed system. The channel is assumed to be multipath and quasi-static for frame duration. There is no wired connection between the transmitting and receiving end. The specifications of the SDR allowed us to ignore negligible signal impairments such as in-phase and quadrature imbalances [103]. The design was converted from a MATLAB Simulink model to the VHDL code, using the Xilinx ISE design suite. The VHDL code was successfully synthesis and mapped for Virtex-6 FPGA under area optimization constraint. All timing and place & route constraints are successfully met. The resource utilization on the FPGA is shown in Table 7. Various parts of the receiver processing-chain are debugged in MATLAB using the Xilinx Chipscope. Xilinx ChipScope Pro tool inserts logic analyzer, system analyzer, and virtual I/O low-profile software cores directly into the design allowing the view to an internal signal or node, including embedded hard or soft processors. Figure 18 shows Chipscope usage with FPGA device, and how it was used to perform soft debugging. Figure 19 shows the receiver constellation from the beginning of time. The constellation gets better at the end of the training period when the receiver is synchronized. The quality of the constellation is assessed at the receiver by

calculating the EVM, which is found approximately 10%. Various other measurements are captured from the MIMO test-bed, which will be presented in future work. We have presented the parameters of our experiment in Table 8.

Table 4.3: Xilinx Resource Estimator for STBC-OFDM design.

Resource (function)	Number of items
Slices	23656 / 74,400
Flip-flops	23641 / 595,200
BRAMs	3869/ 38,304
LUTs	21418 / 476,160
I/O Blocks	326 / 840
DSP48s	237 / 2,016

Table 4.4: Summary of system parameters

Parameter	Value
Power of FPGA design only	<50mW
Symbol rate	20 MSPs
System bandwidth	20 MHz
Intermediate frequency	20 MHz
No. of subcarriers (FFT)	64
Number of data carriers	48
Number of pilot tones	4
Unused subcarriers	12
OFDM symbol duration	32 µs
Length of cyclic prefix	8 symbols
Carrier frequency	2.5 GHz
ADC quantization (default)	14 bits
DAC quantization (default)	16 bits
ADC sampling frequency	250 MSPS
DAC sampling frequency	1 GSPS
The clock speed of SDR	200 MHz
Word length/binary point	16/10
Detectable signal level	-94 dBm

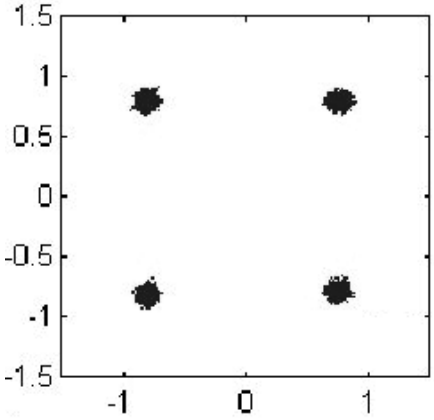

Fig. 4.13. Constellation captured using Xilinx HIL method.

4.8 Conclusion

We have presented a real-time modular implementation of STBC-OFDM on a reconfigurable SDR MIMO testbed. MATLAB simulations and hardware development demonstrated the functionality of our system design. The system supports a 20 MHz bandwidth, a feature in LTE MIMO communication, and works in the ISM band. Our design is modular, portable and scalable for bigger scale. We described in detail the broadband STBC-MIMO test-bed. We described the software development environment and design methodology followed to program STBC-OFDM on the FPGA. Portion of the received data is captured and displayed in Simulink using the RTDX. We have presented preliminary indoor laboratory measurements of our system. Our results confirm working of STBC-OFDM in the 20 MHz bandwidth.

CHAPTER 5: FUTURE RESEARCH DIRECTIONS

There are still a large number of issues and challenges to be investigated in a massive MIMO. Here is the list of possible research directions.

1. User selection (scheduling)

Massive multi-input and multi-output (MIMO) systems, typically using hundreds of base station (BS) antennas to serve tens of users, are widely recognized as a core technique for designing 5G cellular networks [38] [104] [105] [106] [107]. However, given the large number of BS antennas, MIMO systems encounter a dramatic increase in hardware costs and power consumption because each antenna element and radio frequency (RF) chain consists of an RF amplifier and high-resolution data converters, which are the primary power consumers at the BS. Many techniques, such as spatial modulation and hybrid precoding, reduce hardware cost and the energy consumption of the RF chains. Also, the number of users that can be simultaneously served by the BS is limited by the number of selected BS antennas (or the limited RF chains). In this case, users must be scheduled when the number of users is higher than that of the selected BS antennas due to the varying nature of wireless channels. High system performance can be achieved by selecting users with the best channel quality.

2. Unfavourable propagation

Favourable propagation is defined as mutual orthogonality among the vector-valued channels to the terminals and is one of the key properties of the radio channel that is exploited in Massive MIMO. However, there is less research in this

area. Massive MIMO works under favourable propagation environments. However, in practice, there may be propagation environments where the channels are not favourable. For example, in propagation, environments where the numbers of the scatterers are small compared to the numbers of users, or the channels from different users to the BS share some common scatterers, the channel is not favourable. One possibility to tackle this problem is to distribute the BS antennas over a large area.

3. Distributed Massive MIMO

Current research has focused on collocated BS test beds. However, there are significant advantages to massive MIMO systems with non-centralized BSs. Increased spatial diversity is achieved by distributing antennas or remote radio heads, potentially enhancing MIMO's benefits. It is difficult to fit more than 100 antennas into a single array. Distributed Massive MIMO enables more convenient antenna placement, such as spreading them among multiple buildings.

4. Alternative 5G architectures

It would be good to be able to combine Massive MIMO with practical current systems like LTE. In addition, Massive MIMO, small-cells, and mm-wave technology are promising candidates for 5G wireless systems. A good research direction is to design new systems with a combination of these technologies.

4. Intelligent Massive MIMO

With the ever-increasing use of machine intelligence, machine learning (ML) can be used to improve the performance of existing algorithms, achieve close-to-

optimal performance with reduced complexity of implementation [108]. ML will also play an important role in the digital signal processing of the BS baseband processor. For example, deep neural networks could enhance multi-user detection with low-precision ADCs as well as digital pre-distortion for the power amplifiers of the BS [106] [109].

Appendices

The following appendices do not present new contributions. These are added to support the literature discussed in the previous chapters.

Appendix 1

The error vector magnitude (EVM) is used in the Chapter 4. It represents a measure of the deviation of the received symbols from their corresponding ideal position in the constellation plot. The deviation is taken as the Euclidian distance between the ideal symbol coordinate and the actual received symbol. In general, the EVM is averaged over an ensemble of the symbol trajectories and can be defined numerically as

$$EVM = \sqrt{\frac{\sum_{k=1}^{M} |Z(k) - R(k)|^2}{\sum_{k=1}^{M} |R(k)|^2}}$$

EVM provides a measure of the ratio of the error vector to the reference vector. In a perfect system, free of noise and nonlinearities, the measured vector and reference vector would be identical and EVM would be zero. The SNR and EVM of a modulated signal share an inverse relationship. Numerically this relationship can be expressed as,

$$EVM = \frac{1}{\sqrt{SNR} \times L}$$

where L is the coding gain. STBC provides a two-dimensional spatiotemporal encoding to provide diversity gain, without giving any coding gain. Therefore, by measuring the EVM over the desired input signal range, one can readily estimate the SER performance.

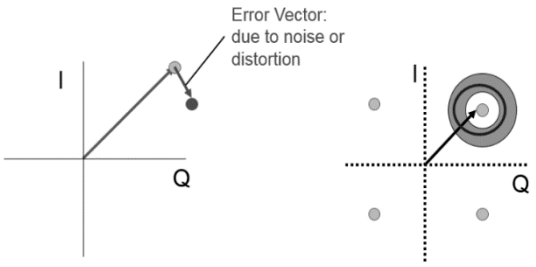

Appendix 2

Antenna selection is discussed in Chapter 2. In order to characterise the radio channel in the urban conditions, the Suzuki distribution was proposed in [110]. The Suzuki distribution describes the scenario when the main wave is subjected to a local scattering by the cluster of buildings, and traverses a path subjected to the influence of multiple reflections and diffractions. The signal is a composition of local path signals at the receiver, because of scattering from the local objects. All the multipath signals have roughly the same delay but different phases. The signal is assumed to have a lognormal strength, since it undergoes the multiplication effects, while the signal distribution is Rayleigh due to an additive scattering effect. The probability density function (PDF) of the Suzuki envelop is described as [110],

$$f_x(x) = \int_0^\infty \frac{x}{\beta^2} \exp\left(\frac{x^2}{2\beta^2}\right) \frac{10}{\ln 10 \sqrt{2\pi}\,\beta\lambda} \exp\left(-\frac{(10\log\beta - \mu)^2}{2\lambda^2}\right) dB$$

The Suzuki process is obtained by the multiplication if the Rayleigh process with lognormal process. We simulated the proposed antenna selection algorithm for various values of the lognormal fading gains. The simulated channel is Suzuki fading channel as in the previous sections. We observe that the capacity of the massive MIMO channel decreases as the lognormal gain increases. The capacity drops by 5 bps/Hz for 8 dB shadow fading gain, compared to the no log-normal fading (i.e. only Rayleigh fading is present). We compared the result of 0dB Suzuki fading with the Rayleigh-only antenna selection algorithm in the Fig.2 to check if the two results coincide with each other. The 0dB Suzuki fading indeed coincides

with the optimal antenna selection algorithm (using exhaustive search) in the Rayleigh-only fading channel.

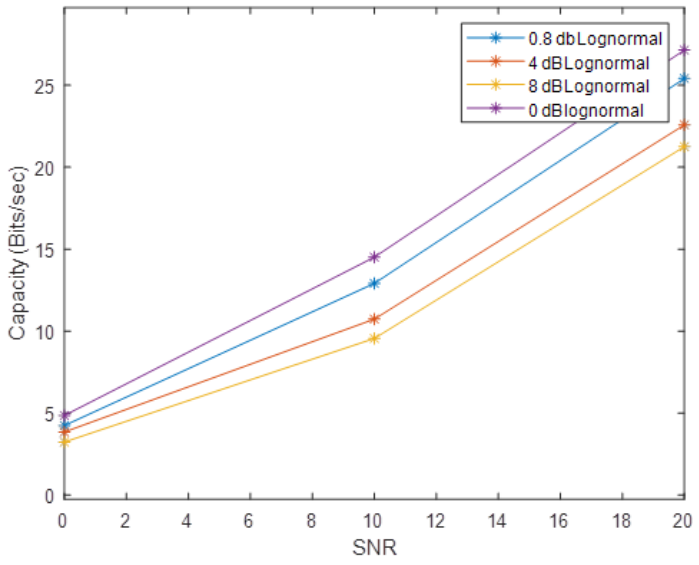

Fig. 1. Effect of lognormal fading on Channel capacity

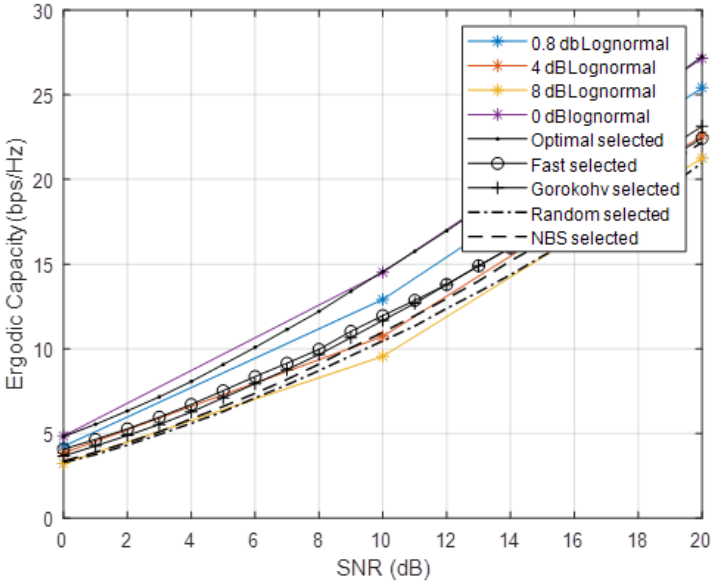

Fig. 2. Comparison of 0dB Suzuki fading to Rayleigh only antenna selection.

Appendix 3

Favourable propagation is defined as mutual orthogonality of vector-valued channels from the base-station to the terminals. This is one of the key properties that is exploited in the Massive MIMO. Favourable propagation of massive MIMO is discussed in the papers [1]. For a MU-MIMO with large arrays, under the favorable propagation conditions, the column-vectors of the propagation matrix are asymptotically orthogonal,

$$\left(\frac{G^H G}{M}\right)_{M \gg K} = D^{1/2} \left(\frac{H^H H}{M}\right)_{M \gg K} D^{1/2} \approx D$$

With a favourable propagation, linear processing can achieve optimal performance. More explicitly, on the uplink, with a simple linear detector such as the matched filter, noise and interference can be cancelled out. On the downlink, with linear beamforming techniques, the base station can simultaneously beam-form multiple data streams to multiple terminals without causing mutual interference [1]. To have the favourable propagation, the radio channels $\{g_k\}$, $k = 1 \ldots K$ are considered pairwise orthogonal if,

$$g_i^H g_i = \begin{cases} 0 & i, j = 1, \ldots K \;\; i \neq j \\ \|g_k\|^2 \neq 0 & k = 1, \ldots, K \end{cases}$$

The above equation is assumed under a perfect scenarios, but can be achieved approximately. According to the law of large numbers, when the number of antennas M grows too large, and $k \neq j$, then. $\frac{1}{M} g_k^H g_i \to 0, \quad M \to \infty$. For this case, we say that the channel is asymptotically favourable.

Appendix 4

This analysis is part of the paper 2 submitted. If the channel is known at the transmitter, the optimum transmit strategy is dirty paper coding, for which the capacity is, e.g.,

$$C = \max_{\{q_k\}} \log_2 \det\left(I_M + p_d H^* D_\beta D_q H\right)$$
$$s.t. \quad q_k \geq 0, \sum_{k=1}^{K} q_k \leq 1 \qquad (1)$$

in which D_q (cf., D_β) is a $K \times K$ real diagonal matrix whose k^{th} element is q_k, representing the transmitted signal power to the kth user. So this formulation fosters optimization of the power allocation (to different users) problem, although power allocation is not pursued further here. This form is known to be a linear programming problem with polynomial time complexity and a global optimum. $\det\left(I_M + AB\right) = \det\left(I_K + BA\right)$, is

$$C = \log_2 \det\left(I_K + \frac{\rho_d K}{N} D_q D_\beta H H^*\right) \qquad (2)$$

The preselection variable, $\Delta_i \quad i = 1, \ldots, M$, is

$$\Delta_i = \begin{cases} 1 & i^{th} \, antenna \, selected, \\ 0 & otherwise \end{cases} \qquad (3)$$

and assembling these as $\mathbf{\Delta} = Diag\{\Delta_1, \Delta_2, .. \Delta_M\}$, with $\mathbf{\Delta}^{\mathrm{H}}\mathbf{\Delta} = \mathbf{\Delta}$ and $\sum_{i=1}^{M} (\Delta_i) = N$, makes (2) into

$$C\left(\mathbf{\Delta}\right) = \log_2 \det\left(I_K + \frac{\rho_d K}{N} D_q D_\beta H \, \mathbf{\Delta} \, H^*\right) \qquad (4)$$

We have maintained the power allocation term in (4), but for the preselection problem, this can be dropped (or alternatively stated, the same power is allocated for now to all the users) by using $D_q = I_K / K$. Equation (4) is known to be convex in Δ_i. The maximization of the capacity can be stated as the optimization problem:

$$\underset{\{\Delta\}}{\text{maximize}} \quad C(\mathbf{\Delta}) = \log_2 \det\left(I_K + \frac{\rho_d}{N} D_\beta H^* \mathbf{\Delta} H \right)$$
$$\text{subject to} \leftrightarrow \quad \Delta_i \in \{0,1\} \qquad (5)$$
$$trace(\Delta) = \sum_{i=1}^{M} \Delta_i = N.$$

This is NP-hard because the Δ_i are binary integer variables but relaxation allows solution in polynomial time. (Linear programming relaxation of the 0-1 integer program is by replacing the constraint that each variable must be 0 or 1, by a weaker constraint such that each variable is within an interval 0 to 1.) So for each constraint, $\Delta_i \in \{0, 1\}$, a pair of linear constraints, viz., $0 \le \hat{\Delta}_i \le 1$, is used instead. The optimization problem is now,

$$\underset{\{\Delta\}}{\text{maximize}} \quad C(\mathbf{\Delta}) = \log_2 \det\left(I_K + \frac{\rho_d}{N} D_\beta H^* \mathbf{\Delta} H \right)$$
$$\text{subject to} \leftrightarrow \quad \Delta_i \in \{0,1\}$$
$$trace(\Delta) = \sum_{i=1}^{M} \Delta_i = N.$$

Our proposed algorithm, based on the Barrier method, is $O(M^{3.})$ for practical purposes, as listed in Table 1. This polynomial time complexity is feasible to solve, including in real-time using a current GPU. We used the MATLAB® Parallel Computing Toolbox which provides Nvidia GPU functions (called CUDA® library) to accelerate the computing.

Algorithm	Complexity
Exhaustive search	$C_N^M N$
Fast algorithm	$O(M^2 K^2)$
Gorrokhov algorithm	$O(NMK)$
NBS algorithm	$O(NM)$
Presented method	$O(M^{3.5})$
Presented method (favorable propagation condition)	$O(M)$

Table . Antenna selection algorithm complexity in MIMO

“Favorable propagation conditions”, means uncorrelated antennas, and with *M*>>*K,* the column-vectors of the channel matrix approach being mutually orthogonal, so that

$$\left(\frac{G\,G^H}{M}\right)_{M\gg K} = D_\beta^{1/2}\left(\frac{H\,H^H}{M}\right)_{M\gg K} D_\beta^{1/2} \approx D_\beta$$

The capacity of a massive MIMO downlink channel simplifies to (cf., (1) with D_q dropped),

$$\begin{aligned} C_{M\gg K} = \ & \log_2 \det\left(I_K + \rho_d\, D_\beta^{1/2} G\, G^H\, D_\beta^{1/2}\right) \\ \approx\ & \log_2 \det\left(I_K + \rho_d\, M D_\beta\right) \\ \approx\ & \sum_{k=1}^{K} \log_2 (1 + M\rho_d\, \beta_k) \end{aligned}$$

There are mainly two interior point methods of linear programming: the primal Newton Barrier Method and the Primal-dual Interior Point Method. The former has complexity $O\left(n^6\right)$ and the latter has complexity $O\left(n^{3.5}\right)$. The primal Newton barrier method requires the initial value to satisfy the primal constraints while the primal-dual interior method requires both primal and dual constraints to be satisfied. The latter is seen as one promising competitor for simplex methods.

REFERENCES

[1] T. Marzetta, E. Larsson, H. Yang and H. Ngo, "Fundamentals of Massive MIMO", Cambridge University Press, 2016.

[2] G. Larsson and et. al., “Massive MIMO for next generation wireless systems,” *IEEE Commun. Mag.,* vol. 52, no. 2, p. 186–195, 2014.

[3] M. Gans and G. Foschini, “On limits of wireless communication in a fading environment when using multiple antennas,” *Wireless Personal Communications,* vol. 6 , no. 3, pp. 311-335, 1998.

[4] M. Schwartz, W. Bennett and S. Stein, "Communication Systems and Techniques", McGraw-Hill, 1966.

[5] R. Vaughan and J. Andersen, "Channels, Propagation and Antenna for Mobile Communications", IEE/Peregrinus, 2003.

[6] R. Heath and et. al., "Foundations of MIMO Communication", Cambridge University Press, 2018.

[7] F. Rusek and et. al., “Scaling up MIMO: Opportunities and challenges with very large arrays,” *IEEE Signal Process. Mag.,* vol. 30, no. 1, pp. 40-60, 2013.

[8] A. Molisch and et. al., “Capacity of MIMO systems with antenna selection,” *in Proc. IEEE ICC*, 2001.

[9] D. Gore and A. Paulraj, “MIMO antenna subset selection with space-time coding,” *IEEE Transactions on Signal Processing,* vol. 50, no. 10, p. 2580–2588, 2002.

[10] Y. Choi and et. al., “Fast algorithms for antenna selection in MIMO systems,” *in Proc. IEEE VTC*, 2003.

[11] S. Sanayei and A. Nostratinia, “Antenna selection in MIMO systems,” *IEEE Communication Magazine,* vol. 42, no. 10, pp. 68-73, 2004.

[12] A. Molish and M. Win, “MIMO systems with antenna selection,” *IEEE Microwave Magazine,* vol. 42, no. 10, pp. 68-73, 2004.

[13] S. Asaad and et. al., “Optimal transmit antenna selection for massive MIMO wiretap channels,” *IEEE Journal on Selected Areas in Communications,* vol. 36, no. 4, 2018.

[14] M. Benmimoune, E. Driouch, W. Ajib and D. Massicotte, “Novel transmit antenna selection strategy for massive MIMO downlink channel,” *The Journal of Mobile Communication, Computation, and Information,* vol. 23, no. 8, pp. 2473-2484, 2017.

[15] M. Benmimoune and e. al., “Joint transmit antenna selection and user scheduling for massive MIMO systems,” *in IEEE WCNC*, 2015.

[16] S. Caban and et. al., “Vienna MIMO testbed,” *EURASIP Journal on Advances in Signal Processing,* 2006.

[17] T. Kaiser, A. Wilzeck and R. Tempel, “A modular multi user testbed,” in *Proc. of IEEE Radio and Wireless Conference*, 2004.

[18] A. Wilzeck and et. al., “MIMO Prototyping Using Sundance's Hardware and Software Products,” Sundance Systems, 2019.

[19] J. Naya, M. Lopez and L. Castedo, “An overview of MIMO testbed technology,” in *Proc. International Symposium on signal, Image, Video and Communications (ISIVC)*, 2008.

[20] O. Bach, N. Bartzoudis, A. Iserte and D. Bueno, “A real-time MIMO-OFDM mobile WiMAX receiver: architecture, design and FPGA implementation,” *The International Journal of Computer and Telecommunications Networking,* vol. 55, no. 16, pp. 3634-3647, 2011.

[21] C. Calero and et. al., “A 2x2 MIMO DVB-T2 system: design, new channel estimation scheme and measurements with polarization diversity,” *IEEE Transactions on Broadcasting,,* vol. 56, no. 2, pp. 184 -192, 2010.

[22] S. Haene and et. al., “A real-time 4-stream MIMO-OFDM transceiver: system design, FPGA implementation and characterization,” *IEEE Journal on Selected Areas in Communications,* vol. 26, no. 6, p. 877–889, 2008.

[23] T. Haustein, and et. al., “Real-time signal processing for multi-antenna systems: algorithms, optimization and implementation on an experimental testbed,” *EURASIP Special Issue on MIMO Implementation Aspects,* 2006.

[24] J. Koivunen and et. al., “Dynamic multi-link indoor mimo measurements at 5.3 GHz,” *in Proc. IEEE EUCAP*, 2007.

[25] N. Czink and et. al., “Can Multi-User MIMO Measurements Be Done Using a Single Channel Sounder?,” COST 2100 TD(08)621, 2008.

[26] Y. Konishi and et. al., “Channel Sounding Technique Using MIMO Software Radio Architecture,” *in Proc. IEEE EUCAP*, 2011.

[27] R. Fernandez and et. al., “Comparison between measurements and simulations of the conventional and distributed MIMO system,” *IEEE Antennas and Wireless Propagation Letters,,* vol. 7, pp. 546-549, 2008.

[28] T. Sorensen and P. Mogensen, “Radio channel measurements on an eight-branch indoor office distributed antenna system,” *in Proc. IEEE VTC*, 2001.

[29] Z. Li and et. al., “Capacity and spatial correlation measurements for wideband distributed MIMO channel in the aircraft cabin environment,” *in Proc. IEEE WCNC*, 2012.

[30] J. Flordelis and et. al., “Measurements of large-scale parameters of a distributed MIMO antenna system in a microcell environment at 2.6 GHz,” *in Proc. IEEE EUCAP*, 2013.

[31] R. Thomä and et. al., “MIMO vector channel sounder measurement for smart antenna system evaluation,” *European Transactions on Telecommunications,* vol. 12, p. 427–438, 2001.

[32] D. Chizhik and et. al., “Multiple-input-multiple-output measurements and modeling in Manhattan,” *IEEE Journal on Selected Areas in Communications,* vol. 21, p. 321–331, 2003.

[33] N. Czink, and et. al., “Stanford July 2008 radio channel measurement campaign,” COST 2100, 2008.

[34] S. Salous, Radio Propagation Measurement, and Channel Modeling, Wiley, 2013.

[35] E. Björnson and et. al., “Massive MIMO for maximal spectral efficiency: How many users and pilots should be allocated?,” *IEEE Trans. Wireless Commun.,* vol. 15, no. 2, p. 1293–1308, 2016.

[36] E. Björnson and et. al., “Massive MIMO systems with non-ideal hardware: Energy efficiency, estimation, and capacity limits,” *IEEE Trans. Inf. Theory,* vol. 60, no. 11, p. 112–7139, 2014.

[37] T. Marzetta, “Noncooperative cellular wireless with unlimited numbers of base station antennas,” *IEEE Trans. Wireless Commun.,* vol. 9, no. 11, p. 3590–3600, 2010.

[38] H. Ngo, “Massive MIMO: Fundamentals and System Designs,,” 2015.

[39] H. Ngo and et. al., “Energy and spectral efficiency of very large multiuser MIMO systems,” *IEEE Trans. Commun.,* vol. 61, no. 4, p. 1436–1449, 2013.

[40] H. Ngo and et. al., “Energy and spectral efficiency of very large multiuser MIMO systems,” *IEEE Trans. Commun.,* vol. 61, no. 4, pp. 1436-1449, 2013.

[41] Y.Yang and et. al., “Performance of conjugate and zeroforcing beamforming in large-scale antenna systems,” *IEEE J. Sel. Areas Commun.,* vol. 31, no. 2, p. 172–179, 2013.

[42] D. Gesbert and et. al., “Shifting the MIMO paradigm,” *IEEE Signal Processing Magazine,* vol. 24, no. 5, pp. 36-46, 2007.

[43] H. Yang and T. Marzetta, “Performance of conjugate and zero-forcing beamforming in large-scale antenna systems,” *IEEE Journal on Selected Areas in Communications, ,* vol. 31, no. 2, pp. 172-179, 2013.

[44] A. Nosratinia and S. Sanayei, “Antenna selection in MIMO systems,” *IEEE Communications Magazine,* vol. 42, no. 10, pp. 68-73, 2004.

[45] J. Proakis, "Digital Communications", McGraw Hill, 2000.

[46] A.F. Molisch, and et. al., “Capacity of MIMO systems with antenna selection,” in *Proc. IEEE ICC*, 2001.

[47] Y. Choi and et. al., “Fast algorithms for antenna selection in MIMO systems,” *in Proc. IEEE ICC*, 2003.

[48] A. Gorokhov, D. Gore and A. Paulraj, “Receive antenna selection for mimo flat-fading channels: theory and algorithms,” *IEEE Transactions on Information Theory,* vol. 49, no. 10, pp. 2687 - 2696, 2003.

[49] A. Gershman and M. Alkhansari, “Fast antenna subset selection in MIMO systems,” *IEEE Transactions on Signal Processing,* vol. 52, no. 2, pp. 339 - 347, 2004.

[50] R. Chen and et. al., “Efficient transmit antenna selection for multiuser MIMO systems with block diagonalization,” *in Proc. IEEE Globecom*, 2007.

[51] M. Mohaisen and K. Chang, “On Transmit Antenna Selection for Multiuser MIMO Systems with Dirty Paper Coding,” *in Proc. IEEE PIMRC*, 2009.

[52] B. Lee and et. al., “An energy-efficient antenna selection for large scale green MIMO systems,” *in Proc. IEEE ISCAS*, 2013.

[53] A. Liu and V. Lau, “Joint power and antenna selection optimization for energy-efficient large distributed MIMO networks,” *in Proc. IEEE ICCS*, 2012.

[54] T. Lan and et. al., “A practical antenna selection technique in multiuser massive MIMO networks,” *IEICE Trans. on Commun.,* vol. E96-B, no. 11, 2013.

[55] H. Li and et. al., “Energy efficiency of large-scale multiple antenna systems with transmit antenna selection,” *IEEE Trans. on Comm,* vol. 62, no. 2, pp. 638-647, 2014.

[56] X. Gao and et. al., “Antenna selection in measured massive MIMO channels using convex optimization,” *in Proc. IEEE Globecom*, 2013.

[57] X. Gao and et. al., “Measured propagation characteristics for very-large MIMO at 2.6 GHz,” *in Proc. ACSSC*, 2012.

[58] X. Gao and et. al., “Multi-Switch for Antenna Selection in Massive MIMO,” *in Proc. IEEE Globecom*, 2015.

[59] X. Gao and et. al., “X. Gao, O. Edfors, F. Rusek, and F. TufvessonLinear pre-coding performance in measured very-large MIMO channels,” *in Proc. IEEE VTC*, 2011.

[60] Y. Pei and et. al., “How many RF chains are optimal for large-scale MIMO systems when circuit power is considered?,” *in Proc. IEEE Globecom*, 2012.

[61] H. Li and et. al., “Energy efficiency of large scale MIMO systems with transmit antenna selection,” *in Proc. IEEE ICC*, 2013.

[62] S. Boyd and L. Vandenberghe, "Convex Optimization", Cambridge University Press, 2004.

[63] A. Dua and et. al., “Receive Antenna Selection in MIMO Systems using Convex Optimization,” *IEEE Trans. Wirel. Commun., ,* vol. 5, no. 9, pp. 2353-2357, 2006.

[64] G.J. Foschini ,“Layered space-time architecture for wireless communication in a fading environment when using multi-element antennas,” *Bell Labs Technical Journal,* 1996.

[65] W. Jakes and D. Cox, "Microwave Mobile Communications", Wiley Press, 1994.

[66] J. Winters, “On the Capacity of Radio Communication Systems with Diversity in a Rayleigh Fading Environment,” *IEEE Journal on Selected Areas in Communications,* vol. 5, no. 5, pp. 871-878, 1987.

[67] A. Saleh, A. Rustako and R. Roman, “Distributed antennas for indoor radio communications,” *IEEE Transactions on Communications,* vol. 35, no. 12, pp. 1245-1251, 1987.

[68] H. Yanikomeroglu and A. Adinoyi, “On the performance of hybrid macro/micro diversity in the reverse-link microcellular networks,” *in Proc. IEEE WCNC*, New Orleans, 2005.

[69] H. Yanikomeroglu and E. Sousa, “CDMA distributed antenna system for indoor wireless communications,” *in Proc. IEEE ICUPC*, 1993.

[70] X. You, and et. al., “Cooperative distributed antenna systems for mobile communications,” *IEEE Wireless Communications Magazine,* vol. 17, no. 3, pp. 35-43, 2010.

[71] A. Paulraj and T. Kailath, “Increasing capacity in wireless broadcast systems using distributed transmission/directional reception”, Patent no. 345599, 1994.

[72] M. Chen and H. Chen, “Capacity of the distributed antenna systems overshadowed fading channels,” *in IEEE VTC*, 2009.

[73] W. Roh and A. Paulraj, “Outage performance of the distributed antennas systems in a composite fading channel,” *in Proc. IEEE VTC*, 2002.

[74] F. Diehm and et. al., “The FUTON Prototype: Broadband Communication through Coordinated Multi-Point using a Novel Integrated Optical/Wireless Architecture,” *in Proc. IEEE Globecom*, 2010.

[75] F. Diehm, P. Marsch and G. Fettweis, “The FUTON prototype: Proof of concept for coordinated multi-point in conjunction with novel integrated wireless/optical architecture,” *in Proc. IEEE WCNC*, 2010.

[76] P. Poutanen, and et. al., “Multi-Link MIMO Channel Modeling Using Geometry-Based Approach,” *IEEE Transactions on Antennas and Propagation,* vol. 60, no. 2, pp. 587-596, 2011.

[77] V. Kolmonen, and et. al., “Measurement-Based Evaluation of Interlink Correlation for Indoor Multiuser MIMO Channels,” *IEEE Antennas and Wireless Propagation Letters,* vol. 9, pp. 311- 314, 2010.

[78] M. Narandzic, and et. al., “On a characterization of large-scale channel parameters for distributed (multi-link) MIMO - The impact of power level difference,” *in Proc. EuCAP*, 2010.

[79] A. Hong and et. al., “Experimental evaluation of correlation properties of large-scale parameters in an indoor LOS environment,” *in Proc. ISWCS*, 2006.

[80] J. Koivunen, P. Almers, V. Kolmonen, J. Salmi, A. Richter, F. Tufvesson, P. Suvikunnas, A. Molisch and P. Vainikainen, “Dynamic multi-link indoor mimo measurements at 5.3 GHz,” *in Proc. EuCAP*, 2007.

[81] Y. Konishi and et. al., “Multi-link Indoor MIMO Measurements at 11 GHz using Scalable Wideband Channel Sounder,” *in Proc. IEEE ISAP*, 2012.

[82] P. Almers, and et. al., “Survey of channel and radio propagation models for wireless MIMO systems,” *EURASIP Journal on Wireless Communications and Networking,* 2007.

[83] M. Hamalainen, A. Nykanen, V. Hovinen and P. Leppanen, “Digital stepping correlator in a wideband radio channel measurement system,” *in Proc. IEEE PIMRC*, 1997.

[84] E. Telatar, “Capacity of multi-antenna Gaussian channels,” *European Transactions on Telecommunications,* vol. 10, no. 6, pp. 585- 595, 1999.

[85] S. Alamouti, “A simple transmit diversity technique for wireless communications,” *IEEE Journal on Selected Areas in Communications,* vol. 16, no. 8, pp. 1451-1458, 1998.

[86] J. Mietzner, R. Schober, L. Lampe, W. Gerstacker and P. Hoeher, “Multiple-antenna techniques for wireless communications - a comprehensive literature survey,” *IEEE Communications Surveys and Tutorials,* vol. 11, no. 2, pp. 87- 105, 2009.

[87] A. Sayed, "Fundamentals of Adaptive Filtering", Wiley, 2003.

[88] H. Ishikawa, “Software-defined radio technology for highly reliable wireless communications,” *Wireless Personal Communications,* vol. 64, no. 3, pp. 461- 472, 2012.

[89] T. Schmidl and D. Cox, “Robust frequency and timing synchronization for OFDM,” *IEEE Transactions on Communications,* vol. 45 , no. 12, pp. 1613-1621, 1997.

[90] V. Nangia and K. Baum, “Experimental broadband OFDM system: field results for OFDM and OFDM with frequency domain spreading,” *in Proc. IEEE VTC*, 2002..

[91] O. Bach, N. Bartzoudis, A. Iserte and D. Bueno, “A real-time FPGA based implementation of a high performance MIMO-OFDM mobile WiMAX transmitter,” *in Proc. WiMob*, 2012.

[92] S. Haene, D. Perils and A. Burg, “A real-time 4-stream MIMO-OFDM transceiver: system design, FPGA implementation and characterization,” *IEEE Journal on Selected Areas in Communications,* vol. 26, no. 6, pp. 877-889, 2008.

[93] Schenk, T. and A. Zelst, “Implementation of a MIMO-OFDM based wireless LAN system,” *IEEE Transactions on Signal Processing,* vol. 52, no. 2, pp. 483-494, 2004.

[94] T. Haustein and et. al., “Real time signal processing for multi-antenna systems: algorithms, optimization and implementation on an experimental testbed,” *EURASIP Special Issue on MIMO Implementation Aspects,* 2005.

[95] G. Stuber, J. Barry, S. Mclaughlin, Y. Li, M. Ingram and T. Pratt, “Broadband MIMO-OFDM wireless communications,” *Proceedings of the IEEE,* vol. 92, no. 2 , pp. 271-294, 2004.

[96] T. Paul and T. Ogunfunmi, “Wireless LAN comes of age: understanding the IEEE 802.11n amendment,” *IEEE Circuits and Systems Magazine,* vol. 8, no. 1, pp. 28-54, 2008.

[97] S. Kay, Fundamentals of statistical signal processing: Estimation and detection theory, Prentice Hall, 1993.

[98] A. Zelst and et. al., “Implementation of a MIMO OFDM based wireless LAN system,” *IEEE Trans. Signal Processing,* vol. 52, no. 2, p. 483–494, 2004.

[99] D. Ramirez, and et. al., “A comparative study of STBC transmissions at 2.4 GHz over indoor channels using a 2×2 MIMO testbed,” *Wireless Communications and Mobile Computing,* vol. 8, no. 9, pp. 1149-1164, 2008.

[100] J. Proakis, "Digital Communications", McGraw Hill, 1989.

[101] H. Prabhu and et. al., “A 60pJ/b 300Mb/s 128x8 Massive MIMO precoder-detector in 28nm FD-SOI,” in *IEEE International Solid-State Circuits Conference*, 2017.

[102] http://www.sdrforum.org, “Software-defined radio forum,” [Online].

[103] L. Perre and et. al., “Efficient DSP and circuit architectures for massive MIMO: State of the art and future directions,” *IEEE Trans. Signal Processing,* vol. 66, no. 18, p. 4717–4736, 2018.

[104] E. Björnson and et. al., “Massive MIMO: Ten myths and one critical question,” *IEEE Commun. Magazine,* vol. 54, no. 2, pp. 114-123, 2016.

[105] E. Björnson, and et. al., “Massive MIMO is a Reality - What is Next? Five Promising Research Directions for Antenna Arrays,” *IEEE Transactions on Signal Processing,* 2019.

[106] F. Boccardi and et. al., “Five disruptive technology directions for 5G,” *IEEE Commun. Mag.,* vol. 52, no. 2, pp. 74-80, 2014.

[107] D. Persson, B. Lau, E. Larsson, T. Marzetta, O. Edfors, F. Tufvesson and F. Rusek, “Scaling up MIMO: Opportunities and challenges with very large arrays,” *IEEE Signal Processing Magazine,* vol. 30, no. 1 , pp. 40-60 , 2013.

[108] J. Andrews and et. al, “What will 5G be?,” *IEEE Journal Sel. Areas in Comm., ,* vol. 32, no. 6, pp. 1065 - 1082, 2014.

[109] E. Björnson and et. al., “Massive MIMO networks: Spectral, energy, and hardware efficiency,” *Foundations and Trends in Signal Processing,* vol. 11, no. 34, pp. 154-655, 2017.

[110] S. Panic and et. al., "Fading and Interference Mitigation in Wireless Communications", CRC Press Ltd, 2017.

[111] N. Zhang and et. al., “A distributed bidirectional wideband MIMO channel sounder,” *in Proc. IEEE HSI*, 2012.

[112] C. Wang, X. Hong, X. Ge, X. Cheng, G. Zhang and J. Thompson, “Cooperative MIMO channel models: A survey,” *IEEE Communications Magazine,* vol. 48, no. 2, pp. 80-87, 2010.

[113] J. Vieira and et. al., “A flexible 100 antenna testbed for massive MIMO,” *in IEEE GLOBECOM*, 2014.

[114] G. Sierksma and Y. Zwols, "Linear and Integer Optimization: Theory and Practice", CRC Press,, 2015.

[115] S. Salous, "Radio Propagation Measurement and Channel Modeling", Wiley, 2013.

[116] F. Rusek and et. al., “Scaling up MIMO: Opportunities and challenges with very large arrays,” *IEEE Signal Process. Mag.,* vol. 30, no. 1, p. 40–46, 2013.

[117] J. Reed, "Software Radio: A modern approach to radio engineering", Prentice Hall, 2002.

[118] A. Nemirovsky and Y. Nesterov, “Interior-point polynomial methods in convex programming,” *Studies in Applied Mathematics,* vol. 13, 1994.

[119] T. Marzetta and et. al., “Noncooperative cellular wireless with unlimited numbers of base station antennas,” *IEEE Trans. Wireless Commun., ,* vol. 9, no. 11, pp. 3590-3600, 2010.

[120] E. Larsson and et. al., “Massive MIMO for next-generation wireless systems,” *IEEE Commun. Mag.,* vol. 52, no. 2, pp. 186-195, 2014.

[121] Y. Konishi, and et. al., “Channel sounding technique using MIMO software radio architecture,” *in Proc. EuCAP*, Rome, 2011.

[122] Y. Konishi, and et. al., “Multi-link indoor MIMO measurements at 11GHz using scalable wideband channel sounder,” *in Proc. IEEE APS*, 2012.

[123] T. Kaiser and et. al., “A modular multi-user testbed,” *in Proc. IEEE RAWCON*, 2004.

[124] J. Naya and et. al., “An overview of MIMO testbed technology,” *in International Symposium on Image/Video Communications*, 2008.

[125] H. Hu, Y. Zhang and J. Luo, Distributed antenna systems: Open architecture for future wireless communications, Auerbach Publications, 2007.

[126] J. Hoydis and et. al., “Massive MIMO in the UL/DL of cellular networks: How many antennas do we need?,” *IEEE Journal Sel. Areas in Comm.,* vol. 31, no. 2, p. 160–171, 2013.

[127] J. Hoydis and et. al., “Channel measurements for large antenna arrays,” *in Proc. ISWCS*, 2012.

[128] P. Harris and et. al., “Performance Characterization of a Real-Time Massive MIMO System with LOS Mobile Channels,” *IEEE Journal on Sel. Areas in Comm.,* vol. 35, no. 6, pp. 1244 - 1253, 2017.

[129] A. Ghosh, R. Ratasuk, B. Mondal, N. Mangalvedhe and T. Thomas, “LTE-advanced: next-generation wireless broadband technology,” *IEEE Transactions on Wireless Communications,* vol. 17, no. 3, pp. 10-22, 2010.

[130] X. Gao and et. al., “X. Gao, O. Edfors, F. Rusek, and F. Tufvesson, "Massive MIMO performance evaluation based on measured propagation data,” *IEEE Trans. Wireless Communications,* vol. 14, no. 7, pp. 3899-3911, 2015.

[131] X. Gao and et. al, “Massive MIMO in real propagation environments: Do all antennas contribute equally?,” *IEEE Transactions on Communications,* vol. 63, no. 11, pp. 3917-392, 2015.

[132] O. Fontbach and et. al., “A real-time MIMO-OFDM mobile WiMAX receiver: architecture, design and FPGA implementation,” vol. 55, no. 16, pp. 3634-3647, 2011.

[133] J. Flordelis and et. al., “Spatial separation of closely-spaced users in measured massive multiuser MIMO channels,” *in Proc. IEEE ICC*, 2015.

[134] B. Fang and et. al., “RAISE: A new fast transmit antenna selection algorithm for massive MIMO systems,” *Wireless Personal Communications,* vol. 80, no. 3, pp. 1147-1157, 2015.

[135] N. Czink, and et. al., “Can multi-user MIMO measurements be done using a single channel sounder?,” COST 2100, 2008.

[136] C. Calero, and et. al., “A 2x2 MIMO DVB-T2 system: design, new channel estimation scheme and measurements with polarization diversity,” *IEEE Transactions on Broadcasting,* vol. 56, no. 2, pp. 184-192, 2010.

[137] S. Caban, and et. al., “Vienna MIMO testbed,” *EURASIP Journal on Advances in Signal Processing,* p. 1–13, 2006.

[138] E. Björnson and et. al, “Massive MIMO has unlimited capacity,” *IEEE Trans. Wireless Commun.,* vol. 17, no. 1, p. 574–590, 2018.